Research Square

Preprints are preliminary reports that have not undergone peer review.
They should not be considered conclusive, used to inform clinical practice,
or referenced by the media as validated information.

Cytogenetic trait evolution and generic boundaries: evidence from Maxillariinae, a recently diversified Neotropical orchid clade

Irene Fátima Vieira Moraes
São Paulo State University — Unesp
Leonardo P. Felix
Federal University of Paraíba — UFPB
Juliano S. Cabral
University of Bonn
Eric C. Smidt
Federal University of Paraná — UFPR
Ana Paula Moraes
ap.moraes@unesp.br

São Paulo State University — Unesp

Research Article

Keywords: chromosome number, CMA/DAPI banding, genome size, heterochromatin, phylogenetic comparative methods

Posted Date: October 14th, 2026

DOI: https://doi.org/10.21203/rs.3.rs-10943628/v1

License: This work is licensed under a Creative Commons Attribution 4.0 International License.
Read Full License

Additional Declarations: No competing interests reported.

Abstract

Orchids are notable for their high diversity in vegetative, floral, and cytogenetic traits. Here we evaluated how cytogenetic traits have evolved and covaried, and assessed their potential contribution to generic delimitation, using Maxillariinae, an important Neotropical clade, as a model. The complete cytogenetic dataset includes chromosome numbers for 107 species and genome size estimates for 67 species, which are interpreted from an evolutionary perspective. Chromosome numbers ranged from 2n = 36 to 2n = 76, with a predominance of counts between 2n = 36 and 2n = 42, consistent with *x* = 20 and recurrent dysploidy detected in the evolutionary analyses. Polyploidy was mainly detected at the population level and was often associated with niche shifts. Genome size appears to be relatively stable in Maxillariinae, with punctual increases and decreases across the phylogeny. Although a marginal effect of heterochromatin block number on genome size variation was detected, PGLS models did not clearly support an association between genome size and any cytogenetic variable. No karyotype trait explained genome size variation; instead, Pagel's λ value close to 1 suggests that genome size varies largely as a consequence of phylogenetic history, possibly reflecting changes in dispersed repetitive DNA sequences rather than changes in chromosome number or heterochromatin distribution alone. Taken together, our cytogenetic analyses, literature survey, and time-calibrated phylogeny provide independent evidence relevant to generic boundaries in Maxillariinae, supporting the recognition of cytogenetically distinct lineages that may be obscured under broadly circumscribed generic concepts.

1 Introduction

Changes in cytogenetic traits (*e.g.*, chromosome number, position and number of heterochromatic bands and rDNA sites, and genome size) play a significant role in plant evolution and diversification (Stebbins, 1971; Mayrose & Lysak, 2021; Benítez-Benítez et al., 2025). In the last decade, studies assessing the main mechanisms involved in karyotype diversification have increasingly integrated species evolutionary histories and phylogenetic comparative approaches, providing a more robust methodological framework for cytogenetic analyses (*e.g.*, Santos et al., 2025; Guerra et al., 2026; Martín-Hernanz et al., 2026) and allowing to infer how cytogenetic traits evolve throughout species evolutionary process and whereas it is potentially associated with different traits (Moraes et al., 2022; Barbosa et al., 2026; Luccetti et al., 2026; Martín-Hernanz et al., 2026).

The recently diversified orchid Neotropical groups, due to its large diversity, stand out as an excellent system for investigating the karyotype evolutionary patterns and potentially associations between cytogenetic traits, and between cytogenetic and ecological traits. Among the recently diversified clades is the species-rich subtribe Maxillariinae (Cymbidieae, Epidendroideae), exhibiting one of the highest speciation rates in Orchidaceae (Zhang et al., 2023; Perez-Escobar et al., 2024). Despite the considerable morphological diversity, Maxillariinae species can be recognized by a conservative basic floral plan with an incumbent anther and four pollinia arranged in two pairs, usually with a larger pollinium attached to a smaller one (Whitten et al., 2000; 2007; Singer & Koehler, 2004; Schuiteman & Chase, 2015; Meneguzzo & Chase, 2025). However, internally, the circumscription of Maxillariinae has undergone substantial

changes over time, based on both anatomical and molecular evidence (Hoehne, 1953, Pabst & Dungs, 1975, Dressler, 1993, Whitten et al., 2000, 2007, Christenson et al., 2012), and its classification continues to undergo profound realignments in the delimitation of genera within the subtribe (Schuiteman & Chase, 2015, Meneguzzo & Chase, 2024).

Concerning cytogenetic traits, diploid chromosome numbers in Maxillariinae varies 1.3-fold (2n = 36 to 46), with some polyploid cytotypes, while genome size varies 3.85-folds (1C = 1.59 pg to 6.12 pg) among diploid species (Amorim-Silva et al., 2026). Maxillariinae taxa present a substantial variation in heterochromatic bands and rDNA sites (e.g., Cabral et al., 2006; Koehler et al., 2008; Moraes et al., 2012; 2016; 2017). Given the recent origin of Maxillariinae and its cytogenetic variability, it is reasonable to hypothesize that these cytogenetic traits retain a strong phylogenetic signal. Additionally, a previous work suggested that genome size in Maxillariinae is associated with habit, with smaller genomes being associated with epiphytism (Moraes et al., 2022), as previously proposed for orchids more broadly (Leitch et al., 2009). Genome-size variation was also associated with the heterochromatin fraction in orchids (Kao et al., 2001; Moraes et al., 2012), and this pattern may also explain the larger genome size variation compared with chromosome number variation observed in Maxillariinae. Unfortunately, Neotropical orchids, despite their available cytogenetic characterization, remain underrepresented in phylogenetic hypotheses, limiting macroevolutionary investigations of chromosome and genome-size evolution (Whitney & Garland Jr., 2010; Barbosa et al., 2026).

In this sense, the present study aims to investigate the mechanisms of cytogenetic evolution in Neotropical orchids using Maxillariinae as a model. This study aims to assess whether cytogenetic traits can provide independent evidence for evaluating generic boundaries in this recently diversified clade and which cytogenetic trait (chromosome number, heterochromatin, and/or rDNA sites) could explain the genome size variation observed in Maxillariinae. To do this, we expanded the representation of cytogenetically characterized Neotropical species in a time calibrated phylogeny and generated and summarized cytogenetic traits (chromosome numbers, heterochromatin banding patterns, rDNA *in situ* hybridization, and genome size data) for the subtribe. Based on our approach, we address the following questions: (1) What are the main mechanisms of karyotype and genome size evolution and the base chromosome number and ancestral state for genome size?, (2) Which cytogenetic trait (chromosome number, heterochromatic blocks, and/or rDNA sites) is correlated with genome size variation?, and (3) Can cytogenetic traits provide independent evidence for assessing generic boundaries in Maxillariinae?

2 Materials And Methods

2.1 Plant Material

New DNA sequences were obtained from 58 specimens (Table S1), while new cytogenetic data were obtained from 22 taxa for karyotype analysis (Table S2), and three species for genome size estimation (Table S2). All specimens were field-collected or provided by private collections and scientific nurseries, including the Frederico Hoehne Orchidarium at the Institute of Environmental Research, São Paulo, Brazil

(hereafter referred to as “FHO”), the Luiz de Queiroz College of Agriculture, University of São Paulo (“ESA”), and the Hannover Botanical Garden (“HAN”). Voucher specimens were deposited in the herbaria EAN, UFP, SP, and HUFABC (abbreviations according to Thiers, 2026). Here, we follow the taxonomic nomenclature proposed by Blanco et al. (2007), as it represents a more detailed taxonomic treatment of Maxillariinae. Nevertheless, Table S1 provides a parallel comparison of the classifications of Blanco et al. (2007) and Meneguzzo & Chase (2024).

2.2 Phylogenetic analysis and estimation of divergence times

Genomic DNA was extracted from 58 specimens representing 45 species following Doyle & Doyle (1987), without β-mercaptoethanol. Sequence amplification was performed using Platinum Taq High Fidelity DNA Polymerase (Invitrogen Life Technologies) and one nuclear (ITS) and four from chloroplast regions (*mat*K, *atp*β-*rbc*L spacer, *rbc*L, and *ycf1*) were amplified with the following primers: 17SE and 26SE for the nuclear ribosomal internal transcribed spacer (ITS) sequences (Sun et al., 1994); 19F and *trn*K2R, with the internal primer 308F used for sequencing, for the plastid gene *mat*K and the flanking region of *trn*K (hereafter referred to as *mat*K; Goldman et al., 2001; Johnson & Soltis, 1994); MaxF and MaxR for the plastid intergenic region *atp*β–*rbc*L spacer (Whitten et al., 2007); *rbc*L_aF and *rbc*L_aR for ribulose-1,5-bisphosphate carboxylase/oxygenase (*rbc*L; Kress & Erickson, 2007); and 3720F and 5500R, with additional internal primers intF and intR used for sequencing, for *ycf*1 (Neubig et al., 2009). PCR reactions followed Whitten et al. (2007) and Neubig et al. (2009), and purification and sequencing were performed by Macrogen (Seoul, South Korea; https://dna.macrogen.com/eng/), using the same primers. A total of 141 new sequences were generated: 34 ITS, 38 *mat*K, 43 *atp*β–*rbc*L, 15 *rbc*L, and 10 *ycf*1 (see asterisks in Table S1).

Additional sequences for the five amplified markers were selected from the GenBank database, prioritizing those that (1) were associated with voucher specimens and (2) exhibited the longest sequence length and highest quality (Table S1). A total of 202 ITS, 225 *mat*K, 168 *atp*β-*rbc*L, 75 *rbc*L, and 109 *ycf*1 sequences were included in the analysis, totaling 931 sequences representing 267 species, covering 25 genera of the Maxillariinae subtribe *sensu* Whitten et al. (2007) and Blanco et al. (2007), and 16 species used as outgroups (Table S1).

Each marker dataset was aligned using Geneious v.7.1.9 (https://www.geneious.com) with the MAFFT v7.017 plugin (Katoh et al., 2018) and trimmed using the smart-gap function implemented in ClipKit (Steenwyk et al., 2020). A concatenated matrix including the five markers was generated using the package ape 5.0 (Paradis et al., 2024). Such a matrix was analyzed under Maximum Likelihood (ML) and Bayesian Inference (BI). For both analyses, the nucleotide substitution model for each partition was selected using the modelTest function (Posada, 2008) from the R package phangorn (Schliep, 2017). The selected models were GTR + I+G4 for ITS, *mat*K, *atp*β-*rbc*L, and *ycf*1, and HKY + I for *rbc*L.

ML analyses were performed in IQ-TREE2 (Minh et al., 2020) with 1,000 ultrafast bootstrap replicates (Hoang et al., 2018), while BI analyses were conducted in MrBayes v.3.2.7 (Ronquist et al., 2012). For BI

analyses, one hot and three cold chains were initiated from random trees to ensure convergence across runs. Each chain ran for 20 million generations, with a sampling frequency of 1,000 generations. Convergence was confirmed when the average standard deviation of split frequencies fell below 0.01, and effective sample sizes (ESS) for each run were checked in Tracer v.1.7.1 (Rambaut et al., 2018). A burn-in of 25% was applied, and trees were summarized in a majority-rule consensus tree, with branch support assessed by posterior probabilities (PP ≥ 0.95 being considered strong; Cummings et al., 2003; Simmons et al., 2004). Phylogenetic conflicts and comparisons between reconstruction methods, ML and BI, were performed using comparePhylo and coPhyloPlot functions from the R package ape (Paradis et al., 2019). The resulting phylogenetic trees were visualised and edited with FigTree v.1.4.4 (https://tree.bio.ed.ac.uk/software/figtree/) and Adobe Photoshop CS5 (Adobe Systems, Inc.).

Divergence times were estimated using secondary calibration points from Givnish et al. (2015) for the divergence between Oncidiinae and Zygopetalinae subtribes, set at 17.45 million years ago (Mya) (95% highest posterior density interval: 14.16–21.15, normal distribution prior, mean = 18, SD = 1.7) and for the crown age of Maxillariinae, set at 13.57 Mya (95% highest posterior density interval: 10.31–17.36, normal distribution prior, mean = 14, SD = 1.8). Divergence times for the Maxillariinae genera were estimated using the same matrix in BEAST 1.10.5 (Suchard et al., 2018). An uncorrelated lognormal relaxed clock model was applied to all partitions, using GTR + I+G4 for ITS, *mat*K, *atp*β-*rbc*L, and *ycf*1, and HKY + I for *rbc*L, with empirical base frequencies for all partitions. The starting tree was the ML phylogeny obtained from IQ-TREE2, with a fixed topology to prevent discrepancies between molecular dating and phylogenetic results. The Yule speciation model (Gernhard, 2008; Pennel & MacPherson, 2025) was used as the tree prior. MCMC chains were run for 1 billion generations, sampling every 1,000 generations. Convergence and effective sample sizes (ESS ≥ 300) were verified in Tracer 1.7.2 (Rambaut et al., 2018) for all parameters. The posterior tree sample was processed in LogCombiner by applying a 25% burn-in and thinning the tree file by retaining one tree every 10 sampled trees, corresponding to one tree every 10,000 generations. A maximum clade credibility tree was subsequently generated in TreeAnnotator.

2.3 Cytogenetic procedures

Chromosome preparation, banding and fluorescent in situ hybridization (FISH) - For chromosome analyses, root tips were pre-treated with 0.002 M 8-hydroxyquinoline at 10°C for 20 hours and processed following Moraes et al. (2012). Selected slides were stained with chromomycin A_3 (CMA) and 4',6-diamidino-2-phenylindole (DAPI) following Schweizer (1976). For in situ hybridization, a D2 probe from *Lotus japonicus* (Pedrosa et al., 2002) and an R2 probe from *Arabidopsis thaliana* (Wanzebock et al., 1997) were used to localise 5S and 35S rDNA loci, respectively, in ten species (Table S2). The FISH protocol followed Moraes et al. (2012). Slides were analyzed under an Olympus BX51 microscope, and selected metaphases were captured with a CCD camera and analyzed using the Image CellSens software (Olympus, Inc.). Images were processed uniformly for contrast and brightness using Adobe Photoshop CS5 (Adobe Systems, Inc.).

Genome size estimation - A similar amount of sample and internal standard (*Vicia faba* ssp. *faba* var. *equina* cv. Inovec; 2C = 26.90 pg; Doležel et al., 1992) fresh leaf tissue were macerated in 0.5 mL of ice-cold Ebihara buffer (Ebihara et al., 2005) with 0.025 µg mL^{-1} RNAse. The nuclear suspension was filtered and stained with 12.5 µL of a 1 mg mL^{-1} propidium iodide solution (PI, Sigma). Analyses were performed using a FACSCanto II flow cytometer (Becton Dickinson, San Jose, CA, USA), kindly made available by the Department of Chemical and Biological Sciences at IBB-UNESP (Botucatu, Brazil). Histograms were generated with FACSDiva software based on 5,000 nuclei (events), and statistical evaluations were conducted using Flowing Software v.2.5.1 (https://www.flowingsoftware.com/). Quality control measurements were based on the coefficient of variation (CV) for each measurement, which was required to be below 5%, and on the standard deviation (SD) and variance among genome size estimates, which were required to be below 3%. These limits ensure that variation observed within and among measurements reflects technical variation rather than intraspecific variation among individuals (Pellicer & Leitch, 2021).

Literature survey - The literature on chromosome number and genome size in Maxillariinae was compiled using the online database OrchidCount (https://orchidcountsdb.epizy.com/; Amorim-Silva et al., 2026). Information on chromosome banding and the localization of 5S and 45S rDNA sites was also recorded based on searches conducted in the Web of Science database for all studies published since 1955 (Table S3). Updated scientific names were confirmed using World Flora Online (https://www.worldfloraonline.org) and the Taxonomic Name Resolution Service (TNRS) v.4 (https://tnrs.iplantcollaborative.org/TNRSapp.html), as well as specialised taxonomic literature.

2.4 Macroevolution: Analyses of cytogenetic traits evolution

Macroevolutionary analyses of cytogenetic traits were performed for the subtribe Maxillariinae based on the ML phylogeny, together with cytogenetic data generated in this study and additional data compiled from the literature. Two pruned phylogenetic trees were generated using drop.tip function from ape package (Paradis et al., 2019) in R (v4.3.0; R Core Team 2025). The first tree included only species with chromosome number data and was used for ancestral chromosome number reconstruction, whereas the second included only species with genome size data and was used for ancestral genome size reconstruction and genome size evolution analyses. All computational analyses were carried out using R, except when otherwise specified.

Chromosome number and karyotype rearrangements - For chromosome number and karyotype rearrangements, we used ChromEvol v.2 (homogeneous models, Mayrose et al., 2010; Glick & Mayrose, 2014) and ChromEvol v.3 (heterogeneous models, Shafir et al., 2025). The best-fitting model, selected based on Akaike Information Criterion (AIC; Akaike, 1974), considering $\Delta AIC \leq 2$ (Burnham & Anderson, 2002), was reanalyzed using 10,000 stochastic simulations to estimate the expected number of chromosome-number changes along branches and to infer ancestral haploid chromosome numbers at selected nodes across the phylogenetic hypothesis. Based on the best-fitting model in ChromEvol v.2,

model adequacy was assessed using the simulation-based framework implemented in the ChromEvol web server (https://chromevol.evolseq.net/), following Rice & Mayrose (2021).

Genome size evolution - The ancestral genome size for Maxillariinae was reconstructed using the fastAnc function from the R package phytools (Revell, 2024). Temporal changes in genome size states was tested using four evolutionary models to evaluate whether genome size evolution is better explained by stochastic divergence (Brownian Motion; Felsenstein, 1973), attraction towards adaptive optima (Ornstein-Uhlenbeck; Butler & King, 2004; Cressler et al., 2015), rapid early diversification (Early Burst; Harmon et al., 2010), or present no association with phylogenetic history (White Noise; Week et al., 2021). The best-fitting model was identified based on the corrected Akaike Information Criterion (AICc; Akaike, 1974), considering $\Delta AIC \leq 2$, using the fitContinuous function from the R package geiger (Pennell et al., 2014). The phylogenetic signal, which reflects the tendency for phylogenetically closely related species to be more similar to each other for a given trait, was estimated with Pagel's λ (Pagel, 1999) and Blomberg's K (Blomberg et al., 2003) indexes using the phylosig function from the R package phytools (Revell, 2024).

Cytogenetic traits associations - To test whether cytogenetic traits explain variation in genome size while accounting for phylogenetic non-independence, we conducted phylogeny-based regressions using Phylogenetic Generalized Least Squares (PGLS) using both pgls function (R package caper; Orme et al., 2023) and likelihood-based generalized least squares models (gls function, R package nlme; Pinheiro et al., 2023), combined with a Pagel's λ correlation structure (corPagel from R package ape; Paradis et al., 2019). Genome size was treated as the response variable, whereas chromosome number, number of heterochromatic blocks, and number of rDNA sites were treated as explanatory variables.

Because cytogenetic traits were not available for all species, univariate PGLS models were fitted using datasets containing the intersection of species for which genome size and the respective predictor were available. To enable direct comparison among alternative predictors, an additional reduced dataset including all cytogenetic traits was assembled, and all competing models were fitted using the same species set and a consistently pruned phylogeny.

For multivariate models, potential collinearity among explanatory variables was assessed using variance inflation factors (VIF function from R package car; Fox et al., 2026). Model support was evaluated using the corrected Akaike Information Criterion (AICc) calculated with the AICc() function from the R package MuMIn (Bárton 2026), considering $\Delta AIC \leq 2$. Parameter estimates and statistical significance were interpreted in conjunction with model comparison results and the estimated strength of phylogenetic signal.

3 Results

3.1 Phylogenetic analysis and divergence times

The concatenated alignment matrix included 267 species and comprised 7,079 aligned nucleotide sites with 3,578 unique sites, 26.5% of missing data, and 1,712 parsimony informative sites. The ML (Fig. 1A and Fig. S1A) and BI (Fig. S1B) trees were largely congruent (Fig. S2). Differences between the analyses mainly involved minor rearrangements among species within genera or shifts in the position of some genera, such as *Brasiliorchis* (Fig. S2). Several dichotomies recovered in ML appeared as polytomies in BI. Consequently, the ML tree contained 266 nodes and the BI tree 230 nodes. In total, 55 clades were recovered only in ML, whereas 19 were recovered only in BI (Fig. S3).

Despite these small differences, both analyses recovered all genera as monophyletic, except *Heterotaxis* and *Nitidobulbon*. *Nitidobulbon proboscideum* was recovered outside the clade comprising the remaining species of *Nitidobulbon* and *Heterotaxis*, whereas the other two *Nitidobulbon* species [*N. cymbidioides* and *N. nasutum*] formed a well-supported clade nested within *Heterotaxis* in both ML and BI trees (Fig. S1).

According to the divergence-time analysis, the crown age of Maxillariinae was estimated at 15.59 Mya (Fig. 1B and Fig. S4). The clade comprising *Hylaeorchis petiolaris*, *Bifrenaria*, *Rudolfiella*, and *Scuticaria*, corresponding to *Bifrenaria* sensu Meneguzzo & Chase (2024) (Group 1 in Table S1), was estimated to have originated at 11.16 Mya. In this clade, two genera of Amazonian origin diversified more recently in the Atlantic Forest, forming distinct clades: *Scuticaria*, which originated at 7.75 Mya in the Amazonian region, diversified in the Atlantic Forest at approximately 4.87 Mya, while *Bifrenaria*, which originated at 6.85 Mya in the Amazonian region and dispersed to and diversified in southeastern Brazil at 3.32 Mya (Fig. S4).

The clade corresponding to *Maxillaria sensu* Meneguzzo & Chase (2024) (Group 2 in Table S1) was estimated to have originated at 13.06 Mya, with 12 out of the 17 genera *sensu* Blanco et al. (2007) showing crown ages between 8 and 6 Mya. The five exceptions were *Cryptocentrum*, the oldest genus in Maxillariinae, with an estimated crown age of 8.58 Mya, and the more recently diversified genera *Rhetinantha* (4.06 Mya), *Sauvetrea* (4.04 Mya), *Mapinguari* (2.54 Mya), and *Cyrtidiorchis* (2.17 Mya). The clade comprising *Xylobium*, *Lycaste*, *Ida*, and *Anguloa* (Group 3 in Table S1) has an estimated crown age of 10.88 Mya and genera crown ages ranging from 4.84 Mya to 2.14 Mya, the latter corresponding to *Anguloa*, the youngest genera in Maxillariinae.

3.2 Cytogenetic characterization

The chromosome numbers of 22 taxa distributed across 11 genera *sensu* Blanco et al. (2007), or three genera *sensu* Schuiteman & Chase (2015) and Meneguzzo & Chase (2024), were determined (Table 1, Figs. 2 and 3). Twelve of the 22 taxa presented here with chromosome number data were also reported in a previous study (Moraes et al., 2022), with the same individuals analyzed in both studies (see PW in Table S3). When combining our data with compiled data from the literature, our complete dataset comprised chromosome numbers for 107 species (Table S3), which presented diploid chromosome number ranging from 2n = 36 to 60, with a prevalence of chromosome numbers between 2n = 36 and 42 (account for 88.03% of all records), with 2n = 40 being the most prevalent chromosome number

(56.41%). Such a tendency could be observed both in the present analyzed species, as in the literature survey. Polyploid cytotypes were described for three species (2.8% of taxa): *Bifrenaria tyrianthina var. magnacalcarata*, *Bif. tetragona*, and *Christensonella subulata*, each presenting cytotypes with 2n = 38 and 2n = 76. *Maxillariella alba*, analyzed here presenting cytotypes of 2n = 40 and 2n = 60, could be considered the fourth species if 2n = 60 represent a triploidy. Dysploid cytotypes were observed in seven species (6.54% of recorded species; Table S3).

Table 1

Cytogenetics results for analysed species. The chromosome number, number and position of heterochromatic bands (CMA and DAPI), and 5S and 45S rDNA sites are presented. Concerning heterochromatic bands and rDNA sites, the number of bands/sites following the position on the chromosome (tr = terminal, px = proximal, int = interstitial) are presented. The table follows the taxonomic proposal of Blanco et al. (2007), and for each genus, the total number of taxa according to Blanco et al. (2007) and/or the World Flora Online database is presented in parentheses.

Species	2n	CMA+	DAPI+	rDNA 5S	rDNA 45S	1Cx (pg)	Fig.
***Brasiliorchis* Singer, Koehler and Carnevali (13)**							
Brasiliorchis consanguinea (Klotzsch) R.B.Singer, S.Koehler and Carnevali+	40	4 px	0	2 int	4 px		3A-B
Camaridium Lindl. (80)							
Camaridium ochroleucum Lindl.	38	2 px + 2 int	2 px				2A
Lycaste Lindl. (51)							
Lycaste aromatica (Graham) Lindl.	40	2 int + 2 tr	0	2 tr	2 tr		3C-D
Maxillaria Ruiz and Pav. (200)							
Maxillaria bradei Schltr. ex Hoehne+	40	2 tr	2 px	2 tr	2 tr		3E-F
Maxillaria crocea Lindl.	40	2 px + 2 tr	6 px				2B
Maxillaria kegelii Rchb.f.	40	2 px + 2 tr	6 px				2C
Maxillaria leucaimata Barb.Rodr.+	40	2 tr	4 px	2 px + 2 tr**	2 tr		3G-H
Maxillaria ochroleuca Lodd. ex Lindl.	40	2 tr	14 px				2D
Maxillaria spiritu-sanctensis Pabst	40	4 int + 2 tr	6 px				2E
Maxillariella Blanco and Carnevali (50)							
Maxillariella alba (Hook.) Blanco and Carnevali	60	4 tr	0				2F
Maxillariella aff. alba (Hook.) Blanco and Carnevali	50	2 px	0				2G
Maxillariella tenuifolia (Lindl.) Blanco and Carnevali+	40	2 px	0				2H

Species	2n	CMA+	DAPI+	rDNA 5S	rDNA 45S	1Cx (pg)	Fig.
***Brasiliorchis* Singer, Koehler and Carnevali (13)**							
Maxillariella variabilis (Bateman ex Lindl.) Blanco and Carnevali+	42	2 px	0	2 px	2 px		3L-M
Mormolyca Fenzl (25)							
Mormolyca ringens (Lindl.) Gentil+	40	4 tr	30 px				2I
Mormolyca rufescens (Lindl.) Blanco+	40	16 px	18–20 px				2J
Nitidobulbon Ojeda, Carnevali and Romero (three species)							
Nitidobulbon nasutum (Rchb.f.) Ojeda and Carnevali+	46	2 int + 4 tr	12 px				2K
Ornithidium Salisb. ex R.Br. (60)							
Ornithidium adendrobium (Rchb.f.) Blanco and Ojeda	38	2 px	0	2 tr	2 px		3I-K
Rhetinantha Blanco (15)							
Rhetinantha cerifera (Barb.Rodr.) Blanco+	38	2 px + 2 int	0				2L
Rhetinantha friedrichsthalii (Rchb.f.) Blanco+	36	2 tr	2 px	4 tr	2 tr		3N-O
Scuticaria Lindl. (9)							
Scuticaria irwiniana Pabst.						5.06	
Scuticaria itirapinensis Pabst.						4.25	
Scuticaria kautskyi Pabst.						10.9	
Scuticaria steelei (Hook.) Lindl.+	40	2 sm px + 38 px*	0	2 int	2 px		3P-Q
Trigonidium Lindl. (7)							
Trigonidium acuminatum Bateman ex Lindl.	40						
		2 tr	0	2 int	2 tr		3R-S
Trigonidium obtusum Lindl.	40	2 tr	0	2 int	2 tr		3T-U

The banding/signal positions are classified as terminal (tr), proximal (px), or interstitial (in).

* duplicated proximal DAPI+ bands, one in each chromosome arm

**duplicated 5S rDNA sites indicated by the presence of two sites in the same chromosome arm.

+' indicate specimens already analysed on Moraes et al. (2022) for chromosome number

A considerable variation in heterochromatic banding patterns was observed among the 22 taxa analyzed (Table 1, Figs. 2 and 3). All taxa showed GC-rich heterochromatic blocks (CMA^+ bands) and 11 taxa also presented AT-rich proximal heterochromatic blocks ($DAPI^+$ bands). While CMA^+ bands varied in both number and chromosomal position, $DAPI^+$ bands were consistently located in proximal regions and varied only in number (Fig. 4).

The most common pattern was two CMA^+ band pairs, detected in 11 taxa (50%) and located in proximal and/or terminal positions (Fig. 4), followed by four CMA^+ band pairs, detected in seven taxa (31.8%). The highest number of CMA^+ bands was observed in *Scuticaria steelei* (2n = 40; Fig. 3P), which presented one pair of large proximal CMA^+ bands and minor heterochromatic bands on all other chromosomes. This species also differs from all other Maxillariinae genera by its large chromosomes, measuring approximately 5–6 µm (Fig. 3P–Q). Proximal distended CMA^+ bands were observed in four taxa: *Camaridium ochroleucum* (2n = 38; Fig. 2A), *Brasiliorchis consanguinea* (2n = 40; Fig. 3A), *Mor. rufescens* (Fig. 2J), and *Ornithidium adendrobium* (2n = 38; Fig. 3I–K). Among the 18 surveyed genera (Table S3), CMA^+ bands were typically located in terminal regions, whereas $DAPI^+$ bands, detected in 37 species from ten genera, were most commonly located in proximal regions (83.33%). Only six species (16.67%) showed terminal $DAPI^+$ bands, and one species, *Rudolfiella aurantiaca*, presented both terminal and proximal $DAPI^+$ bands.

The most common pattern for the 5S rDNA sites in present study (Table 1 and Figs. 3 and 4B) was one pair. Among the ten analyzed species, two exhibited two pairs of 5S rDNA: *Max. leucaimata* with four sites occur on a single chromosome pair (Fig. 3G-H) and *Rhe. friedrichsthalii* with two pairs of 5S rDNA sites on two separate chromosome pairs(Fig. 3N-O). Considering the 35S rDNA sites, it is always co-localized with CMA^+ band and the present data suggest that the most common pattern is a single terminal pair (Fig. 3; Table 1), in agreement with the pattern observed when the full dataset is considered (Table S3): c. 60% of species present one site pair and 69.4% present terminal sites.

The literature survey retrieved data for 38 species, totalizing information for 48 species when combined with the present dataset (Table S3). The most common pattern for 5S rDNA was also a single pair of sites (45.61%; Table S3). A higher number of site pairs were observed in 18 species with 15 species presenting two pairs, *Rud. aurantiaca* with three pairs, *Tri. egertonianum* with four pairs and *Brasiliorchis porphyrostele* presenting three sites (one homomorphic and one heteromorphic pair). The position of 5S rDNA sites was variable, with 45.61% located at the terminal position, 28.07% at the interstitial position, and 26.07% of sites at the proximal position. However, when well-sampled genera were considered, a consistent positional pattern emerged. For example, *Bifrenaria* (44.4% of the genus sampled) presented 5S rDNA sites predominantly at the proximal position, *Brasiliorchis* (76.9%) predominantly at the terminal

position, and *Christensonella* (45.5%) predominantly at the interstitial position (Table S3). A recurrent chromosome rearrangement affecting 5S rDNA sites involved site duplication, resulting in two sites on the same chromosome, one located proximally and the other at the interstitial or terminal position detected in five species from five different genera (Table S3). The number of 35S rDNA sites was less variable than that of 5S rDNA: 29 species (60.42%) presented one pair of sites and 18 species (37.50%) presented two pairs, whereas *Brasiliorchis ubatubana* presented five pairs. The chromosomal position of 35S rDNA sites was also less variable, with 69.4% located at the terminal position and 30.6% at the proximal position, and no interstitial sites observed.

The genome size was determined for three *Scuticaria* species: *Scu. irwiniana* Pabst, 1C = 5.06 pg; *Scu. itirapinensis* Pabst, 1C = 4.25 pg; and *Scu. kautskyi* Pabst, 1C = 10.90 pg (Table 1 and Table S3). Combining literature records with the data obtained here, genome size estimates were available for 67 species and varied nearly sevenfold, from 1C = 1.59 pg in *Tri. acuminatum* to 1C = 10.93 pg in *Scu. kautskyi* (Table S3), both species presenting 2n = 40. Despite the large variability and large genomes, the average 1C-value for Maxillariinae is 1C = 3.45 ± 1.35 pg (Table S3).

3.3 Macroevolution - Analysis of character evolution.

Considering the punctual differences detected between both phylogenetic reconstruction methods, the macroevolution analyses were performed using the ML phylogenetic tree which showed a low number of politomies.

3.3.1 Chromosome number and genome size evolution and ancestral reconstruction

The analysis using ChromEvol v.2 suggested x = 20 as the base chromosome number for subtribe Maxillariinae (Fig. 5), which was conserved in 80% of genera (Table 2). The best fitting model was Constant Rate Demi; however, considering the ΔAIC ≤ 2, this model cannot be clearly distinguished from Linear Rate Demi and Constant Rate Demi Est (Table S4). These models assume ascending and descending dysploidy, duplication and demi-duplication in very similar rates (Table S4); however, whereas the two former models assume duplication and demi-duplication at the same rate, the last assumes that these events occur at independent rates. The difference between the two former models lies in the rate of chromosome number change: while the constant-rate model assumes that changes occur independently of the current chromosome number, the linear-rate model allows changes to depend on its current value.

ChromEvol v.3, which allows heterogeneous models, inferred the model without rate shifts (*i.e.*, equivalent to the homogeneous model) as the most suitable, with karyotype change rates consistent with those obtained using ChromEvol v.2 (Table S4). In both analyses, ascending and descending dysploidy were the most frequent rearrangements, particularly descending dysploidy. However, the base chromosome number inferred by ChromEvol v.3 was *x* = 18 for Maxillariinae, but matched ChromEvol v.2

ancestral base number for all genera (Table 2). The very low rate of base number transitions indicates that this shift is negligible for Maxillariinae (Table 2 and Table S4).

Table 2

Compilation of cytogenetic data for Maxillariinae genera based on a literature survey combined with new data obtained in this study. For each genus with more than one species sampled in the phylogeny and with available chromosome number and genome size data, we report the genera total number of species, following Blanco et al. (2007), the number of species with chromosome number and genome size data reported (with sampling percentages), and the estimated ancestral base chromosome number and genome size.

Genus	**Total Number of Species**	**Sampled Species with Chromosome Number (%)**	**Base Chromosome Number (*x*)**	**Sampled Species with Genome Size (%)**	**Ancestral Reconstruction of Genome Size (1C, in pg)**
Anguloa Ruiz & Pav.	14	3 (21.40)	20	2 (14.3)	3.72
Bifrenaria Lindl.	23	10 (43.50)	19	7 (30.4)	3.67
Brasiliorchis Singer, Koehler & Carnevali	13	12 (92.30)	20	10 (76.9)	3.7
Camaridium Lindl.	80	4 (5)	20	3 (3.7)	2.73
Christensonella Szlach., Mytnik, Górniak & Smiszek	12	8 (66.70)	18	8 (66.7)	2.41
Heterotaxis Lindl. / *Nitidobulbon* Ojeda, Carnevali & Romero	13 / 3	8 (61.5) / 1 (33.3)	20	6 (46.15) / 0	3.22
Lycaste Lindl.	51	12 (23.53)	20	3 (5.88)	3.26
Maxillaria Ruiz & Pav.	200	11 (4.40)	20	4 (2)	2.57
Maxillariella Blanco & Carnevali	50	8 (16)	20	4 (8)	2.83
Mormolyca Fenzl, Denkschr.	25	2 (8)	20	2 (8)	2.89
Ornithidium Salisb. ex R.Br.	60	6 (10)	20	2 (3.3)	*
Rhetinantha Blanco	15	4 (26.70)	19	2 (13.35)	2.86
Scuticaria Lindl.	12	2 (16.67)	20	5 (41.67)	3.94
Trigonidium Lindl.	7	4 (57.10)	20	4 (57.10)	2.63

Genus	Total Number of Species	Sampled Species with Chromosome Number (%)	Base Chromosome Number (*x*)	Sampled Species with Genome Size (%)	Ancestral Reconstruction of Genome Size (1C, in pg)
Xylobium Lindl.	39	4 (10.26)	20	3 (7.69)	3.83

Since the best-fitting models showed similar support and karyotype change rates, model adequacy was assessed using the Constant Rate Demi homogeneous model. Good performance was observed for Variance (p = 0.31) and Shannon's entropy (p = 0.07), indicating that simulated chromosome numbers fall within parameter space and that chromosome numbers are relatively homogeneously distributed across the phylogeny (Table S5). The last two parameters, related to Parsimony, both showed p = 0.0 (Table S5), suggesting that the model overestimates the number of chromosomal changes across the phylogeny and through time.

The ancestral genome size of Maxillariinae was estimated at 1C = 3.74 pg, with a tendency toward genome size reduction throughout the phylogeny (Fig. 5, Table 2). Punctual increases were observed in *Scuticaria* and specific terminals inside *Brasiliorchis* (Fig. 5).

3.3.2 Evolutionary mode and trait evolution of genome size

Three evolutionary models were tested, Brownian Motion (BM), Ornstein–Uhlenbeck (OU), and Early Burst (EB), along with the White Noise model (WN), used as a non-phylogenetic null model (Table S6). BM and OU were the best-fitting models ($\Delta AIC \leq 2$); however, the α parameter in the OU model was estimated as zero, indicating that the OU process collapses to BM. Both Blomberg's K and Pagel's λ indicated strong phylogenetic signal (K = 0.589 and λ = 0.999, respectivelly; Table S6).

3.3.3 Associations among karyotypic traits and genome size

To test which karyotype traits are associated with genome size and may explain its variation, the relationships between genome size and three karyotype traits are tested. The karyotype variables showed no evidence of collinearity (variance inflation factors: 1.17, 1.16, and 1.03 for chromosome number, number of heterochromatic blocks, and number of rDNA sites, respectively); therefore, both univariate and multivariate models were evaluated. Univariate and multivariate PGLS analyses yielded inconsistent results depending on the implementation used.

In univariate analyses, models including karyotype predictors did not outperform the null model (Table S7) indicating that chromosome number, heterochromatin block number, and rDNA site number do not explain additional variation in genome size beyond phylogenetic effects. Even considering a small dataset composed only of species with data for the four karyotype traits, no model outperformed the null model (Table S8).

In contrast, multivariate PGLS analyses implemented using the pgls function detected an effect of heterochromatin block number on genome size variation in Maxillariinae ($p = 0.034$; Table S9). However, this effect was not supported by likelihood-based generalized least squares models (gls with Pagel's λ). Likelihood-based GLS models showed better performance than pgls-based models ($\Delta AICc = 36.45$). Such results reinforce the conclusion that karyotype traits do not independently explain genome size variation in this clade, in agreement with univariate PGLS analyses.

In all models, Pagel's λ was estimated at or near 1, indicating a strong phylogenetic signal in genome size and suggesting that most of the observed variation is explained by shared evolutionary history rather than by the tested cytogenetic predictors (Fig. 4).

4 Discussion

In the present study, we obtained karyological and genome size data for 25 taxa (22 and three taxa, respectively) across 11 genera of the subtribe Maxillariinae (*sensu* Blanco et al., 2007). Additionally, we compiled published chromosome number data (now available for 107 species) and genome size data (now available for 67 species) for the group. Based on this combined dataset and in the light of a new time calibrated phylogeny, we modeled chromosome number and genome size evolution, estimating ancestral states for both traits. These approaches allowed us to assess karyotype and genome size diversity within Maxillariinae, evaluating whether genome size variation could be explained by other cytogenetic traits or its variation is explained by Maxillariinae evolutionary history and if cytogenetic traits are taxonomically informative to elucidate Maxillariinae genera boundaries.

4.1 Maxillariinae phylogeny and divergence times

Our results largely agree with Whitten et al. (2007), and the few differences detected are mainly associated with polytomies described by the latter. Almost all genera were recovered as monophyletic in both studies, with the main difference being the recovery of *Nitidobulbon* nested within *Heterotaxis* in the present study.

The small genus *Nitidobulbon* has already been considered part of *Heterotaxis* due to its morphological similarity and could be misidentified as *Heterotaxis*, especially when only vegetative material is available (Ojeda et al., 2003; 2009). Phylogenetic analyses have recovered *Nitidobulbon* as monophyletic using both morphological data and nuclear ITS marker (Ojeda et al., 2003; Moraes et al., 2017), but as nested within *Heterotaxis* when chloroplast markers were used, as observed here. Even with our sampling, when only the ITS marker was used, *Nitidobulbon* was recovered as monophyletic (Fig. S5). Such differences between nuclear and chloroplast markers suggest potential hybridization between genera (Moraes et al., 2016), reflecting the close relationship between *Nitidobulbon* and *Heterotaxis*.

Despite its importance in the Neotropical epiphytic stratum, Maxillariinae has been poorly represented in biogeographic studies and time-calibrated phylogenies. Based on limited sampling, crown age estimates for Maxillariinae have varied widely among studies (Gustafsson et al., 2010; Givnish et al., 2016; Pérez-

Escobar et al., 2017; Serna-Sánchez et al., 2021). Nevertheless, more recently, Zhang et al. (2023) estimated the crown age of Maxillariinae at 11.62 Mya and suggested a recent diversification during Late Miocene epoch (Neogene Period), presenting one of the highest diversification rates among Neotropical epiphytes, as also suggested by Pérez-Escobar et al. (2024). The crown age estimates of Zhang et al. (2023) are broadly consistent with ours, although slightly younger for the three main clades: *Bifrenaria* sensu Meneguzzo & Chase (2024), 9.02 Mya (7.93–9.14 Mya) versus 11.23 Mya here; *Maxillaria* sensu Schuiteman & Chase (2015), 8.67 Mya (8.21–8.94 Mya) versus 13.10 Mya here; and the clade comprising *Xylobium*, *Lycaste*, *Ida*, and *Anguloa* (*Lycaste* sensu Meneguzzo et al., 2022), 9.43 Mya (8.84–9.96 Mya) versus 10.94 Mya here. Therefore, despite differences in absolute age estimates, previous studies and the present analysis consistently support Maxillariinae as a relatively young lineage that experienced rapid evolutionary radiation during the Neogene Period, with genera diversifying mainly in the last 8 to 6 Mya.

Overall, the information generated here establishes the evolutionary context needed to interpret the mechanisms underlying karyotype and genome-size evolution, and lineage boundaries in Maxillariinae based on multiple evidences. The recent origin of the subtribe, together with its high diversification rate, suggests that many of the present chromosomal rearrangements observed occurred over a relatively short evolutionary interval.

4.2 Karyotype diversity in Maxillariinae

The subtribe Maxillariinae shows a conserved chromosome number ranging from 2n = 36 to 60, both in the new data presented here and in the literature survey. Considering the ten taxa not included in Moraes et al. (2022; Table S3), for four taxa this is the first report of chromosome number [*Maxillaria ochroleuca*, *Max. spiritu-sanctensis* (both with 2n = 40), *Maxillariela aff. alba* (2n = 50), and *Ornithidium adendrobium* (2n = 38)] and four species showed the same chromosome number as previously reported in the literature [*Lycaste aromatica*, *Maxillaria crocea* Lindl., *Trigonidium acuminatum*, and *Tri. obtusum*, all with 2n = 40; Table S3]. The two remaining species differed from those reported in the literature: *Maxillariela alba* (2n = 60 here *vs.* 2n = 40; Blumenschein & Paker, 1963) and *Camaridium ochroleucum*, with a dysploid variation (2n = 38 here *vs.* 2n = 40; Blumenschein and Paker, 1963).

The origin of the cytotypes reported here for *Maxillariella alba* (2n = 40 and 2n = 60) may represent a polyploid cytotype, representing one of the four species with polyploid cytotypes described in the subtribe. The other three polyploid cytotypes represent species that exhibit niche divergence by changing habit from epiphytic to obligatory or facultative lithophytic habit. For example, *Bifrenaria tyrianthina var. magnacalcarata* is the only species in the genus exclusively rupicolous, whereas the remaining *Bifrenaria* species are predominantly epiphytic (Koehler et al., 2004; Moraes et al., 2017). The morphological differences between epiphytic and rupicolous populations led Frederico Hoehne (1950) to propose two varieties of *Bif. tetragona*: *Bif. tetragona var. umbrophila* and *B. tetragona var. rupicola*, both currently treated as heterotypic synonyms of *B. tetragona* (2n = 38/76). Similarly, *Christensonella subulata* (2n = 38/76) occurs preferentially on rocky outcrops and is the only species of the genus also recorded in mountain savannas with rocky outcrops, an environment characterized by high solar radiation, water

deficit, and shallow soils (Koehler et al., 2012). Such a shift away from the ecological niche of diploid counterparts is commonly associated with polyploid success.

Despite the well-established role of polyploidy as a major driver of plant evolution (Heslop-Harrison et al., 2023), including in different orchids lineages (Del Prete et al., 1991; D'Emerico et al., 2005; Cordeiro et al., 2018), in Maxillariinae, polyploidy seems to have a limited role, with polyploid cytotypes primarily associated with intraspecific variation (Felix & Guerra, 2000; Koehler et al., 2008; Moraes et al., 2016; 2017; 2022) and environmental heterogeneity, raising the possibility that polyploidy is linked to local adaptation in distinct ecological contexts (e.g., Grünig et al., 2024; Mortier et al., 2024; Lu et al., 2025; Pungaršek et al., 2026). Indeed, niche shifts, through the associated environmental stress, may promote a higher frequency of unreduced gametes, thereby favoring polyploid formation (Ramsey & Schemske, 1998; Soltis et al., 2003; Parisod et al., 2010; Van der Peer et al., 2021). The niche shifts may evolve as a consequence of geographical differentiation after polyploidy rather than as direct adaptations to environmental stress (Clo et al., 2022; Kauai et al., 2026). Additionally, considering the recent Maxillariinae, mostly between 8 and 6 Mya, the low frequency of polyploid species may be associated with the absence of major geological disturbances which could promote ancient large-scale whole genome duplication events (Van de Peer et al., 2021; Chen et al., 2026).

However, delayed effects of older genome duplication events could still be shaping the evolution of this clade, especially through dysploidy, which is one of the most common mechanisms in the diploidisation process (Mayrose & Lysak, 2021; Li et al., 2021). Finally, niche shifts could be observed in the three Maxillariinae species with polyploid cytotypes; however, *Maxillariella alba* (2n = 60) showed no apparent change in habit or distribution compared with its related diploid cytotype.

4.3 Dysploidy as the main mechanism shaping karyotype in Maxillariinae

Dysploidy seems to play a central role in chromosome evolution in this group, as well as in angiosperms (Carta et al., 2020). Here, the importance of dysploidy is reflected in the observed data and supported by karyotype evolution analyses performed using ChromEvol (v.2 and v.3), as well as the chromosome banding pattern and in situ localization of 5S and 35S rDNA. The convergence among these different lines of evidence strongly indicates that karyotype evolution in Maxillariinae is driven primarily by structural rearrangements associated with ascending and descending dysploidy, rather than by genome duplication events.

The basic number (*x*) suggested to Maxillariinae *s.l.* is *x* = 20/18, which agrees with the widely observed 2n = 40 throughout the subtribe and also largely found within the subtribe Stanhopeinae (Felix & Guerra, 2000), the sister clade to Maxillariinae (Whitten et al., 2000). The frequent dysploidy observed in the subtribe can be found both in generic and infrageneric levels. For example, among the fifteen analyzed genera with more than three species sampled, only four genera showed a stable diploid chromosome number, whereas ten genera exhibited dysploid variation (either dysploid species and/or dysploid cytotypes).

The extensive variation in heterochromatin banding patterns revealed by CMA/DAPI in Maxillariinae, as observed in *Christensonella* (Koehler et al., 2008) and *Heterotaxis* (Moraes et al., 2017), as well as in other orchid groups, as in *Paphiopedilum* (Cox et al., 1998; Lan et al., 2011) illustrate the importance of centric fusion-fission as the source of the observed ascendent dysploidy tendency (Jones, 1998; Perry et al., 2004). Nevertheless, in the case of *Cam. ochroleucum* analyzed here, the dysploidy difference (2n = 38 *vs.* 2n = 40) could be suggested as a consequence of technical error, since distended constrictions may favour erroneous chromosome counts by conventional staining. Chromosome number determinations that rely solely on conventional techniques may yield erroneous results, since distended regions often do not stain. Hence, to confirm undocumented or ambiguous chromosome counts reported in the literature, techniques such as heterochromatin banding are desirable, as they ensure that distended heterochromatic blocks are stained and detectable, allowing not only the correct chromosome number determination, as the identification of chromosome rearrangements involved in dysploid variation.

Also the rDNA localization can reveal structural chromosome rearrangements. The most common organization of 5S and 35S rDNA in plants is two sites for both markers, with 5S preferentially located in proximal positions, whereas 35S is commonly located in terminal positions (Roa & Guerra 2012; 2015; Garcia et al., 2017). Our results agree with those previously suggested by these authors, except for the recurrent terminal position of 5S rDNA in Maxillariinae.

An atypical 5S rDNA organization with two 5S rDNA sites on the same chromosome was observed in five Maxillariinae species, suggesting a structural rearrangement, such as a chromosome inversion. However, such rearrangements can be favored by the known association between rDNA sites (both 5S and 35S rDNA) and transposable elements (TE; Garcia et al., 2024). TEs may carry rDNA fragments, affecting the number and position of rDNA sites by mobilizing them across the genome or promoting structural rearrangements through recombination (Garcia & Gaiesky, 2015). For example, the TEs Cassandra, En/Spm-like, and Ty1-copia-like elements are found commonly associated to 5S rDNA (Kalendar et al., 2008; Raskina et al., 2004), with the former presenting a mimic of 5S rDNA promoter sequence in its LTR region (Maiwald et al., 2024). These TEs could favour the origin of new rDNA sites on the same chromosome or on different chromosomes, as detected in some Maxillariinae species. Multiple 35S rDNA sites may likewise have been favored by TE–rDNA associations, which could have promoted the spread of rDNA sites across the genome in orchids, as suggested in *Paphiopedilum* (Lan et al., 2011; Garcia et al., 2024). In this sense, TE-mediated displacement of rDNA sequences could partially explain the diversity of 5S and 35S rDNA patterns observed in Maxillariinae, both by moving sequences across the genome and by promoting structural chromosomal rearrangements.

4.4 Genome size diversity and evolution in Maxillariinae

According to Leitch et al. (2010), the genome size in Maxillariinae should be considered small (median 1C = 3.38 pg and mean 1C = 3.45 pg). The ancestral genome size for the subtribe and for the genera are similar, with lineage-specific reductions and increases detected across the subtribe. The genome size variation reflects the karyotype evolutionary history, with its dysploid and polyploid events, as well as the

accumulation/excision of repetitive DNA (Bhadra et al., 2023). Considering species with stable chromosome number, the genome size increase reflects a higher amplification than excision rate, which is suggested to be particularly observed in species with 1C ≥ 10 pg. Depending on the organization of the repetitive sequences, such sequences could be detected as heterochromatic blocks, as already observed in plants (e.g., *Capsicum*; Park et al., 2011) and animals (such as bats; Volleth et al., 2023). In orchids, a direct correlation between heterochromatic blocks and genome size was detected in *Phalaenopsis* (Kao et al., 2001) and in *Brasiliorchis* (Moraes et al., 2012). Taking into account the sevenfold genome size variation in Maxillariinae, along with a robust phylogeny and a large karyotype characterization dataset, it is possible to discuss the origin of genome size variation: whether it is caused by changes in chromosome number (dysploid and/or polyploid) or by repetitive DNA expansion, and if such expansion could be detected as heterochromatic blocks and/or rDNA sites.

The best-fitting model, Brownian Motion, suggests that genome size evolves through the gradual accumulation of small and random changes along the phylogeny and it was already suggested as the best-fitting model for genome size in a sample of Maxillariinae orchids (Moraes et al., 2022). The present results agree with the strong phylogenetic signal detected ($\lambda = 0.999$), indicating that closely related species tend to exhibit similar genome sizes, as commonly observed in different angiosperm groups (Ortiz et al., 2026; Barbosa et al., 2026) and reinforce the assumption that phylogenetic comparative methods are mandatory when studying trait evolution and associations (Whitney and Garland Jr., 2010; Barbosa et al., 2026). The alpha value ($\alpha = 0$) indicates no detectable attraction towards an evolutionary optimum, which makes the Ornstein-Uhlenbeck model converge to Brownian Motion, suggesting that genome size diversification is better explained by phylogenetic history than by stabilizing selection around a particular value. However, Ornstein-Uhlenbeck model outperformed Brownian Motion in an alternative orchid sample (Trávníček et al., 2019) and other plant groups (e. g., Bromelioideae; Paule et al., 2020).

4.5 Are karyotype traits associated with genome size?

The overall effect of karyotype traits on genome size variation reveals no association with chromosome number, probably due to the low rate of polyploidy in the subtribe and the lower effect of recurrent dysploidy, which changes chromosome number but, usually, does not affect genome size in a substantial manner. Decoupling between chromosome number and genome size has already been suggested (Carta et al., 2020; Martín-Hernanz et al., 2026). However, the weak association between genome size and heterochromatin blocks was detected, but it was restricted to a single multivariate PGLS implementation and was not supported by information-theoretic model comparison. In this sense, such a result should be interpreted as a method-dependent artifact rather than robust evidence of an association, not supporting the suggested correlation between genome size and heterochromatic blocks as previously suggested (Kao et al., 2011; Moraes et al., 2012; Volleth et al., 2023), but agreeing with literature which did not find correlation between maize genome size and knob heterochromatin (Realini et al., 2021), neither rDNA sites number (Barbosa et al., 2026). Consistent with this interpretation, genome size variation in Maxillariinae likely reflects variation in the repetitive DNA fraction dispersed throughout the

genome rather than organized into heterochromatic blocks or rDNA sites, following the tendency observed in different groups of plants and animals (Potapenko et al., 2026, Zhao et al., 2025). In Maxillariinae, the genus *Scuticaria* illustrates this pattern.

Despite presenting the largest genome sizes in the subtribe, all *Scuticaria* species present 2n = 40, the most common chromosome number in Maxillariinae, reinforcing the limited role of numerical karyotype changes in genome size evolution within the subtribe. Furthermore, the *Scuticaria* species analyzed so far do not present large heterochromatic blocks on their chromosomes; however, their chromosomes are two to four times longer than the average chromosome of the other genera, suggesting that the accumulated repetitive sequences are spread throughout the karyotype, increasing the chromosome size as observed in *Helianthemum* (Martín-Hernanz et al., 2026), rather than organized into distinct blocks, as detected in *Brasiliochis schunkeana* (Moraes et al., 2012). Together, these results indicate that genome size evolution in Maxillariinae is largely decoupled from karyotype traits as chromosome number variation, heterochromatic blocks and/or rDNA sites and may be driven primarily by lineage-specific changes in dispersed repetitive DNA content, making this DNA fraction an important mechanism driving genome evolution in Maxillariinae.

4.6 Insights on Maxillariinae generic boundaries based on cytogenetic traits

Generic boundaries in Maxillariinae have been the subject of intense taxonomic debate in recent decades, often alternating between approaches that recognize smaller, more homogeneous lineages (splitting proposals by Whitten et al., 2007; Blanco et al., 2007) and more conservative proposals that recognize a small number of broadly circumscribed genera (lumping as suggested by Schuiteman & Chase, 2015; Meneguzzo & Chase, 2024). Although both approaches only recognized monophyletic groups, they may differ in how well they reflect the biological diversity and evolutionary history of the lineages. For example, Schuiteman & Chase (2015) suggested further enlarging the original megagenus *Maxillaria*, arguing that a single megagenus would be easily morphologically diagnosable by its one-flowered inflorescence and non-plicate leaves. On the other hand, many taxonomists, since Hoehne (1947), have argued that smaller clades make scientific names more predictive of taxon traits, thereby making communication more informative.

The recent origin and one of the highest speciation rates in Orchidaceae suggested to Maxillariinae, and especially to *Maxillaria*, just reinforce how challenging it could be to define the taxonomic limits (Pérez-Escobar et al., 2024). However, taking all together, our complete dataset, comprising more than one hundred species, many of them characterized by chromosome banding and rDNA localization, suggested that different lineages present distinct karyotypic patterns. For example, considering the four well-sampled genera (with more than 40% of their species analyzed), such a combination of cytogenetic traits seems to reveal genus-specific cytogenetic patterns, suggesting that the megagenus *Maxillaria* groups independent evolutionary lineages. Therefore, although both lumping and splitting approaches are possible since both approaches recover monophyletic groups, the broad lumping approach may

group cytogenetically distinct evolutionary lineages and reduce the biological informativeness of generic names.

5 Conclusion

Taken together, our karyological, genome-size, and phylogenetic data provide a framework for interpreting cytogenetic evolution in Maxillariinae and assessing its relevance to generic boundaries. Our results suggest that, from an ancestral condition of $x = 20$ and a relatively small genome, Maxillariinae karyotypes were shaped primarily by recurrent dysploidy, whereas polyploidy played a more limited role, mostly at the population level, and may be associated with niche shifts. The complete cytogenetic dataset, comprising more than one hundred species, many characterized by chromosome banding and rDNA loci, indicates that different lineages have distinct karyotypic profiles. Genome-size variation appears to be largely decoupled from chromosome number and heterochromatin blocks, and may instead reflect changes in dispersed repetitive DNA. These results provide independent cytogenetic evidence relevant to generic boundaries in Maxillariinae, supporting the recognition of cytogenetically distinct lineages that may be obscured under broadly circumscribed generic concepts. The recent origin and rapid diversification inferred for Maxillariinae, especially within *Maxillaria s.l.*, further highlight the difficulty of defining generic limits in the subtribe. Thus, although broader taxonomic circumscriptions may be nomenclaturally acceptable, they may also group distinct evolutionary lineages and reduce the biological informativeness of generic names.

Declarations

6 Acknowledgements

The authors would like to thank Dr Boris Schlumpberger, Nandino Baillot, and Ulrike Gessert, from the Hannover Botanical Garden, as well as Prof Dr Samantha Koehler, Dr Eduardo Catharino, and Dr Fábio de Barros, from the orchid collections of the Luiz de Queiroz College of Agriculture, University of São Paulo (ESALQ) and the Institute for Environmental Research of São Paulo, for providing access to the plant material used in this study.

I.F.V.M. acknowledge scholarship received from Conselho Nacional de Desenvolvimento Científico e Tecnológico (CNPq 142376/2025-6). J.S.C. acknowledges scholarships received from the Brazilian Agencies CNPq and Fundação de Amparo à Ciência e Tecnologia do Estado de Pernambuco (FACEPE). L.P.F. acknowledges CNPq within the scope of PELD - Paraíba (Process 445968/2024-9). E.C.S. and A.P.M. acknowledge CNPq for research productivity grant (processes 405493/2021-5 and 312855/2021-4 to E.C.S. and 314642/2020-0 to A.P.M.). A.P.M. acknowledge Fundação de Amparo à Ciência e Tecnologia do Estado de São Paulo (FAPESP, Process 2022/05890-3). I.F.V.M. and A.P.M. are affiliated with the Center for Research on Biodiversity Dynamics and Climate Change (CEPID FAPESP#2021/10639-5). The Article Processing Charge for the publication of this research was funded by the Coordenação de Aperfeiçoamento de Pessoal de Nível Superior - Brasil (CAPES).

Author Contributions

Designed the research: A.P.M. and L.P.F. Data analysis: I.F.V.M., J.S.C. and A.P.M. Collection: A.P.M. Interpretation: I.F.V.M., J.S.C., L.P.F., E.C.S., and A.P.M. Writing the manuscript: I.F.V.M. and A.P.M. All authors revised the manuscript and approved the final version.

Conflict of Interest

The authors declare no conflicts of interest.

Data availability

The concatenated alignment, maximum-likelihood and Bayesian phylogenetic trees, dated tree, cytogenetic datasets, genome-size data, and R scripts used in this study are available from ScienceDB under 10.57760/sciencedb.43869 and/or from GitHub at https://github.com/PlantCytogenomics/Maxillariinae. Newly generated sequences have been deposited in GenBank under the accession numbers listed in Table S1.

References

1. Akaike H. 1974. A new look at the statistical model identification. *IEEE Transactions on Automatic Control* 19: 716–723.
2. Amorim-Silva JJ, Santos RR, Cardoso MIO, Moraes AP. 2026. A comprehensive review of cytogenetic data of Epidendroideae (Orchidaceae): the OrchidCounts, a new database as a tool for evolution studies. *Plant Systematics and Evolution* 312:3.
3. Barbosa SG, Sattler MC, Nardino M, Olivoto T, Yotoko K. 2026. Historical shifts and ecological patterns: rethinking genome size evolution in *Coffea* L. *Journal of Evolutionary Biology* 39: 865–877.
4. Bartoń K. 2026. MuMIn: Multi-Model Inference. CRAN: Contributed Packages.
5. Benítez-Benítez C, Mohan A v., Sánchez-Villegas R, Gómez-Ramos I, Valdés-Florido A, Lucek K et al. 2025. Bridging micro and macroevolution: insights from chromosomal dynamics in plants. *Frontiers in Plant Science* 16: 1606450.
6. Bhadra S, Leitch IJ, Onstein RE. 2023. From genome size to trait evolution during angiosperm radiation. *Trends in Genetics* 39: 728–735.
7. Blanco MA, Carnevali G, Whitten WM, Singer RB, Koehler S, Williams NH, Ojeda I, Neubig KM, Endara L. 2007. Generic realignments in *Maxillariinae* (Orchidaceae). *Lankesteriana* 7: 515–537.
8. Blomberg SP, Garland T, Ives AR. 2003. Testing for phylogenetic signal in comparative data: Behavioral traits are more labile. *Evolution* 57: 717–745.
9. Blumenschein A, Paker IU. 1963. Número de cromossomas nas Maxillariinae (Orchidaceae). *Ciência e Cultura* 15: 255.
10. Burnham KP, Anderson DR. 2002. *Model selection and multimodel inference: A Practical Information-Theoretic Approach*, 2°. New York: Springer.

11. Butler MA, King AA. 2004. Phylogenetic comparative analysis: A modeling approach for adaptive evolution. *The American Naturalist* 164: 683.
12. Cabral JS, Felix LP, Guerra M. 2006. Heterochromatin diversity and its co-localization with 5S and 45S rDNA sites in chromosomes of four *Maxillaria* species (Orchidaceae). *Genetics and Molecular Biology* 664: 659–664.
13. Carta A, Bedini G, Peruzzi L. 2020. A deep dive into the ancestral chromosome number and genome size of flowering plants. *New Phytologist* 228: 1097–1106.
14. Chen H, Almeida-Silva F, Logghe G, Maere S, Bonte D, van de Peer Y. 2026. The rise of polyploids during environmental upheaval. *Cell* 189: 3608–3622.e5.
15. Christenson E, Harding PA, McIllmurry M, Blanco MA. 2012. *Maxillaria*: An unfinished monograph, 1st ed.
16. Clo J, Padilha-Gracía N, Kolár F. 2022. Polyploidization: Consequences of genome doubling on the evolutionary potential of populations. *American Journal of Botany* 109: 1213–1220.
17. Cordeiro JMP, Nollet F, Buril MT, Chase MW, Felix LP. 2018. A new species of Gomesa (Oncidiinae, orchidaceae) from inselbergs in Brazilian caatinga: Morphological and karyological evidence. *Phytotaxa* 374: 147–154.
18. Cox A v., Abdelnour GJ, Bennett MD, Leitch IJ. 1998. Genome size and karyotype evolution in the slipper orchids (Cypripedioideae: Orchidaceae). *American Journal of Botany* 85: 681–687.
19. Cressler CE, Butler MA, King AA. 2015. Detecting adaptive evolution in phylogenetic comparative analysis using the Ornstein-Uhlenbeck model. *Systematic Biology* 64: 953–968.
20. Cummings MP, Handley SA, Myers DS, Reed DL, Rokas A, Winka K. 2003. Comparing bootstrap and posterior probability values in the four-taxon case. *Systematic Biology* 52: 477–487.
21. D'Emerico S, Pignone D, Bartolo G, Pulvirenti S, Terrasi C, Stuto S, Scrugli A. 2005. Karyomorphology, heterochromatin patterns and evolution in the genus *Ophrys* (Orchidaceae). *Botanical Journal of the Linnean Society* 148: 87–99.
22. Dolezel J, Sgorbati S, Lucretti S. 1992. Comparison of three DNA fluorochromes for flow cytometric estimation of nuclear DNA content in plants. *Physiologia Plantarum* 85: 625–631.
23. Dornelas CSM, Silva RS, Alencar J, Felix LP, Buril MT, Nollet F. 2026. Different clades, different changes: karyotype evolution in Convolvulaceae, with emphasis on *Jacquemontia* and the phylogenetic placement of *Daustinia montana*. *Botanical Journal of the Linnean Society* 00: 1–9.
24. Doyle JJ, Doyle JL. 1987. A rapid DNA isolation procedure for small quantities of fresh leaf tissue. *Phytochemical Bulletin* 19: 11–15.
25. Dressler LR. 1993. Phylogeny and classification of the orchid family, 1°. Cambridge: Cambridge University Press.
26. Ebihara A, Ishikawa H, Matsumoto S, Lin SJ, Iwatsuki K, Takamiya M, Watano Y, Ito M. 2005. Nuclear DNA, chloroplast DNA, and ploidy analysis clarified biological complexity of the *Vandenboschia*

radicans complex (Hymenophyllaceae) in Japan and adjacent areas. *American Journal of Botany* 92: 1535–1547.

27. Felix LP, Guerra M. 2000. Cytogenetics and cytotaxonomy of some Brazilian species of Cymbidioid orchids. *Genetics and Molecular Biology* 23: 957–978.
28. Felix LP, Guerra M. 2010. Variation in chromosome number and the basic number of subfamily Epidendroideae (Orchidaceae). *Botanical Journal of the Linnean Society* 163: 234–278.
29. Felsenstein J. 1973. Maximum likelihood estimation of evolutionary trees from continuous characters. *American Journal of Human Genetics* 25: 471–492.
30. Fox J, Weisberg S, Price B. 2026. car: Companion to Applied Regression. CRAN: Contributed Packages.
31. Garcia CF, Gaiesky VLS. 2015. Evolução cromossômica em eucariotos – rearranjos cromossômicos e elementos de transposição. In: Carareto CMA, Monteiro-Vitorello CB, van Sluys MA eds. *Elementos de transposição: diversidade, evolução, aplicações e impacto nos genomas dos seres vivos*. Rio de Janeiro: Sociedade Brasileira de Genética / Editora Fiocruz. 43–64.
32. Garcia S, Kovařík A, Leitch AR, Garnatje T. 2017. Cytogenetic features of rRNA genes across land plants: analysis of the Plant rDNA database. *Plant Journal* 89: 1020–1030.
33. Garcia S, Kovarik A, Maiwald S, Mann L, Schmidt N, Pascual-Díaz JP, Vitales D, Weber B, Heitkam T. 2024. The dynamic interplay between ribosomal DNA and transposable elements: A perspective from genomics and cytogenetics. *Molecular Biology and Evolution* 41: msae025.
34. Gernhard T. 2008. The conditioned reconstructed process. *Journal of Theoretical Biology* 253: 769–778.
35. Givnish TJ, Spalink D, Ames M, Lyon SP, Hunter SJ, Zuluaga A et al. 2015. Orchid phylogenomics and multiple drivers of their extraordinary diversification. *Proceedings of the Royal Society B: Biological Sciences* 282: 20151553.
36. Givnish TJ, Spalink D, Ames M, Lyon SP, Hunter SJ, Zuluaga A et al. 2016. Orchid historical biogeography, diversification, Antarctica and the paradox of orchid dispersal. *Journal of Biogeography* 43: 1905–1916.
37. Glick L, Mayrose I. 2014. ChromEvol: Assessing the pattern of chromosome number evolution and the inference of polyploidy along a phylogeny. Molecular Biology and Evolution 31: 1914–1922.
38. Goldman DH, Freudenstein J, Kores PJ, Molvray M, Jarrell DC, Whitten WM, Cameron KM, Jansen RK, Chase MW. 2001. Phylogenetics of Arethuseae (Orchidaceae) based on Plastid *mat*K and *rbc*L Sequences. *Systematic Botany* 26: 670–695.
39. Grünig S, Patsiou T, Parisod C. 2024. Ice age-driven range shifts of diploids and expanding autotetraploids of Biscutella laevigata within a conserved niche. New Phytologist 244: 1616–1628.
40. Guerra M, Vaio M, Nascimento J, Santana W, Santos A, Lima DF, Felix LP, Fiaschi P. 2026. Deep karyotypic and genomic changes drive the evolution of *Oxalis* subgenus *Thamnoxys* (Oxalidaceae). *Annals of Botany* 137: 2133–2157.

41. Gustafsson ALS, Verola CF, Antonelli A. 2010. Reassessing the temporal evolution of orchids with new fossils and a Bayesian relaxed clock, with implications for the diversification of the rare South American genus *Hoffmannseggella* (Orchidaceae: Epidendroideae). *BMC Evolutionary Biology* 10: 177–190.
42. Harmon LJ, Losos JB, Jonathan Davies T, Gillespie RG, Gittleman JL, Bryan Jennings W, Kozak K, McPeek M, Moreno-Roark F, Near T, Purvis A, Ricklefs R, Schluter D, Schulte J, Seehausen O, Sidlauskas B, Torres-Carvajal O, Weir J, Mooers A. 2010. Early bursts of body size and shape evolution are rare in comparative data. *Evolution* 64: 2385–2396.
43. Heslop-Harrison JS, Schwarzacher T, Liu Q. 2023. Polyploidy: its consequences and enabling role in plant diversification and evolution. *Annals of Botany* 131: 1–9.
44. Hoang DT, Chernomor O, von Haeseler A, Minh BQ, Vinh LS. 2018. UFBoot2: Improving the ultrafast bootstrap approximation. *Molecular Biology and Evolution* 35: 518–522.
45. Hoehne FC. 1947. Reajustamento de algumas espécies de Maxillarieas do Brasil, com a criação de dois novos gêneros para elas. *Arquivos de Botânica do Estado de São Paulo* 2: 65–73.
46. Hoehne FC. 1950. Registo de novas variedades de *Bifrenaria* do Brasil. *Arquivos de Botânica do Estado de São Paulo* 2: 116–117.
47. Hoehne FC. 1953. Flora Brasilica - Orchidaceae, 1°. São Paulo: Instituto de Botânica.
48. Johnson LA, Soltis DE. 1994. Matk DNA-sequences and phylogenetic reconstruction in Saxifragaceae s. str. *Systematic Botany* 19: 143–156.
49. Jones K. 1998. Robertsonian fusion and centric fission in karyotype evolution of higher plants. *The Botanical Review* 64: 273–289.
50. Kalendar R, Tanskanen J, Chang W, Antonius K, Sela H, Peleg O, Schulman AH. 2008. Cassandra retrotransposons carry independently transcribed 5S RNA. *Proceedings of the National Academy of Sciences* 105: 5833–5838.
51. Kao YY, Chang SB, Lin TY, Hsieh CH, Chen YH, Chen WH, Chen CC. 2001. Differential accumulation of heterochromatin as a cause for karyotype variation in *Phalaenopsis* orchids. *Annals of Botany* 87: 387–395.
52. Katoh K, Rozewicki J, Yamada KD. 2018. MAFFT online service: Multiple sequence alignment, interactive sequence choice and visualization. *Briefings in Bioinformatics* 20: 1160–1166.
53. Kauai F, van de Peer Y, Bonte D. 2026. Ecological opportunity and the onset of polyploid niche expansion waves. *Proceedings of the National Academy of Sciences* 123: e2522071123.
54. Koehler S, Amaral MCE. 2004. A taxonomic study of the South American genus *Bifrenaria* Lindl. (Orchidaceae). *Brittonia* 56: 314–345.
55. Koehler S, Cabral JS, Whitten WM, Williams NH, Singer RB, Neubig KM, Guerra M, Souza AP, Amaral MCE. 2008. Molecular phylogeny of the neotropical genus *Christensonella* (Orchidaceae, Maxillariinae): Species delimitation and insights into chromosome evolution. *Annals of Botany* 102: 491–507.

56. Koehler S, Singer RB, Carmo M, Amaral E. 2012. Taxonomic revision of the neotropical genus *Christensonella* (Maxillariinae, Orchidaceae). *Botanical Journal of the Linnean Society* 168: 449–472.
57. Lan T, Albert VA. 2011. Dynamic distribution patterns of ribosomal DNA and chromosomal evolution in *Paphiopedilum*, a lady's slipper orchid. *BMC Plant* Biology 11:126–141.
58. Leitch IJ, Beaulieu JM, Chase MW, Leitch AR, Fay MF. 2010. Genome Size Dynamics and Evolution in Monocots. *Journal of Botany* 2010: 1–18.
59. Leitch IJ, Kahandawala I, Suda J, Hanson L, Ingrouille MJ, Chase MW, Fay MF. 2009. Genome size diversity in orchids: consequences and evolution. *Annals of Botany* 104: 469–481.
60. Lu WX, Tu WQ, Chen D, Wang ZZ, Guo YP. 2025. Niche shifts and localized competitive dynamics influence the persistence and distribution of polyploids in the genus *Achillea* (Asteraceae). *Annals of Botany* 135: 963–976.
61. Maiwald S, Mann L, Garcia S, Heitkam T. 2024. Evolving Together: Cassandra retrotransposons gradually Mirror Promoter Mutations of the 5S rRNA Genes. *Molecular Biology and Evolution* 41: msae010.
62. Martín-Hernanz S, Albaladejo RG, Viruel J, Matos R, Lopes SB, Rubio E et al. 2026. Genome size evolution in *Helianthemum* (Cistaceae): Dynamic genomes within a conserved chromosomal framework. *Molecular Phylogenetics and Evolution* 221: 108627.
63. Mayrose I, Barker MS, Otto SP. 2010. Probabilistic models of chromosome number evolution and the inference of polyploidy. *Systematic Biology* 59: 132–144.
64. Mayrose I, Lysak MA. 2021. The evolution of chromosome numbers: Mechanistic models and experimental approaches. *Genome Biology and Evolution* 13.
65. Meneguzzo TEC, van den Berg C, Chase MW. 2022. Proposal to conserve the name *Lycaste* against *Anguloa* and *Xylobium* (Orchidaceae). *Taxon* 71: 475–476.
66. Meneguzzo TEC, Chase MW. 2024. An enlarged circumscription of *Bifrenaria* (Orchidaceae: Maxillariiinae). *Phytotaxa* 638: 143–154.
67. Minh BQ, Schmidt HA, Chernomor O, Schrempf D, Woodhams MD, von Haeseler A, Lanfear R, Teeling E. 2020. IQ-TREE 2: New models and efficient methods for phylogenetic inference in the genomic era. *Molecular Biology and Evolution* 37: 1530–1534.
68. Moraes AP, Engel TBJ, Forni-Martins ER, de Barros F, Felix LP, Cabral JS. 2022. Are chromosome number and genome size associated with habit and environmental niche variables? Insights from the Neotropical orchids. *Annals of Botany* 130: 11–25.
69. Moraes AP, Koehler S, Cabral JS, Gomes SSL, Viccini LF, Barros F, Felix LP, Guerra M, Forni-Martins ER. 2017. Karyotype diversity and genome size variation in Neotropical Maxillariinae orchids. *Plant Biology* 19: 298–308.
70. Moraes AP, Leitch IJ, Leitch AR. 2012. Chromosome studies in Orchidaceae: Karyotype divergence in Neotropical genera in subtribe Maxillariinae. *Botanical Journal of the Linnean Society* 170: 29–39.

71. Moraes AP, Simões AO, Alayon DIO, de Barros F, Forni-Martins ER. 2016. Detecting mechanisms of karyotype evolution in *Heterotaxis* (Orchidaceae). *PLoS ONE* 11: 1–18.
72. Neubig KM, Whitten WM, Carlsward BS, Blanco MA, Endara L, Williams NH, Moore M. 2009. Phylogenetic utility of *ycf*1 in orchids: A plastid gene more variable than *mat*K. *Plant Systematics and Evolution* 277: 75–84.
73. Ojeda I, Carnevali G, Williams NH, Whitten WM. 2003. Phylogeny of the *Heterotaxis* Lindley complex (Maxillariinae): Evolution of the vegetative architecture and pollination syndromes. *Lankesteriana* 7: 45–47.
74. Ojeda I, Germán CFC, Gustavo ARG. 2009. *Nitidobulbon*, a new genus of maxillariinae (Orchidaceae). *Novon* 19: 96–101.
75. Orme D, Freckleton R, Thomas G, Petzoldt T, Fritz S, Isaac N, Pearse W. 2023. Caper: Comparative analyses of phylogenetics and evolution in R. CRAN: Contributed Packages 1–36.
76. Ortiz AM, Chalup L, Silvestri MC, Samoluk SS, Lavia GI, Seijo G. 2026. Evolution of genome size in Arachis (Fabaceae): a history linked to chromosomal dynamics and dispersal across the South American seasonally dry diagonal. *Botanical Journal of the Linnean Society (in press)*.
77. Pabst GFJ, Dungs F. 1975. *Orchidaceae brasilienses*. 1° ed. Hildesheim: Brucke verlag Kurt Schmersow.
78. Pagel M. 1999. Inferring the historical patterns of biological evolution. *Nature* 401: 877–884.
79. Paradis E, Schliep K. 2019. Ape 5.0: An environment for modern phylogenetics and evolutionary analyses in R. *Bioinformatics* 35: 526–528.
80. Parisod C, Holderegger R, Brochmann C. 2010. Evolutionary consequences of autopolyploidy. *New Phytologist* 186: 5–17.
81. Park M, Jo SH, Kwon JK, Park J, Ahn JH, Kim S et al. 2011. Comparative analysis of pepper and tomato reveals euchromatin expansion of pepper genome caused by differential accumulation of Ty3/Gypsy-like elements. *BMC Genomics* 12.
82. Paule J, Heller S, Maciel JR, Monteiro RF, Leme EMC, Zizka G. 2020. Early diverging and core Bromelioideae (Bromeliaceae) reveal contrasting patterns of genome size evolution and polyploidy. *Frontiers in Plant Science* 11: 1295.
83. Pedrosa A, Sandal N, Stougaard J, Schweizer D, Bachmair A. 2002. Chromosomal map of the model legume *Lotus japonicus*. *Genetics* 161: 1661–1672.
84. van de Peer Y, Ashman TL, Soltis PS, Soltis DE. 2021. Polyploidy: an evolutionary and ecological force in stressful times. *Plant Cell* 33: 11–26.
85. Pellicer J, Powell RF, Leitch IJ. 2021. The application of flow cytometry for estimating genome size, ploidy level endopolyploidy, and reproductive modes in plants. In: Besse P ed. *Methods in Molecular Biology*. Humana Press Inc. 325–361.
86. Pennell MW, Eastman JM, Slater GJ, Brown JW, Uyeda JC, Fitzjohn RG, Alfaro ME, Harmon LJ. 2014. Geiger v2.0: An expanded suite of methods for fitting macroevolutionary models to phylogenetic

trees. *Bioinformatics* 30: 2216–2218.

87. Pennell M, MacPherson A. 2025. Reading Yule in light of the history and present of macroevolution. *Philosophical Transactions of the Royal Society B: Biological Sciences* 380: 20230299.
88. Pérez-Escobar OA, Bogarín D, Przelomska NAS, Ackerman JD, Balbuena JA, Bellot S et al. 2024. The origin and speciation of orchids. *New Phytologist* 242: 700–716.
89. Pérez-Escobar OA, Chomicki G, Condamine FL, Karremans AP, Bogarín D, Matzke NJ, Silvestro D, Antonelli A. 2017. Recent origin and rapid speciation of Neotropical orchids in the world's richest plant biodiversity hotspot. *New Phytologist* 215: 891–905.
90. Perry J, Slater HR, Choo KHA. 2004. Centric fission - simple and complex mechanisms. *Chromosome Research* 12: 627–640.
91. Pessoa EM, Araújo AM, Barberena FFVA, Batista JAN, Benelli AP, Bento JSP et al. 2025. An Overview of Orchidaceae from Brazil: Advances and Shortfalls After 400 Years of Studies. *Plants* 14: 3520–3580.
92. Pinheiro J, Bates D. 2026. nlme: linear and nonlinear mixed effects models. CRAN: Contributed Packages.
93. Posada D. 2008. jModelTest: Phylogenetic model averaging. *Molecular Biology and Evolution* 25: 1253–1256.
94. Potapenko E, Shermeister B, Mandel T, Hübner S. 2026. Intraspecific genome size variation is attributed to adaptive silencing of transposable elements in *Hordeum species*. *Molecular Biology and Evolution* 43: 1–16.
95. del Prete C, Mazzola P, Miceli P. 1991. Plant systematics karyological differentiation and speciation in mediterranean *Anacamptis* (Orchidaceae). *Plant Systematics and Evolution* 174: 115–123.
96. Pungaršek Š, Dolenc Koce J, Frajman B. 2026. Importance of polyploidisation for diversification of hyperdiverse *Euphorbia subgen. Esula*: polyploidy is positively correlated with increasing latitude, but negatively with elevation. *Annals of botany* 00: 1–21.
97. R Core Team. 2025. R: A Language and Environment for Statistical Computing.
98. Rambaut A, Drummond AJ, Xie D, Baele G, Suchard MA. 2018. Posterior summarization in Bayesian phylogenetics using Tracer 1.7. *Systematic Biology* 67: 901–904.
99. Ramsey J, Schemske DW. 1998. Pathways, mechanisms, and rates of polyploid formation in flowering plants. *Annual Review of Ecology and Systematics* 29: 467–501.
100. Raskina O, Belyayev A, Nevo E. 2004. Activity of the En/Spm-like transposons in meiosis as a base for chromosome repatterning in a small, isolated, peripheral population of *Aegilops speltoides* Tausch. *Chromosome Research* 12: 153–161.
101. Realini MF, Poggio L, Cámara-Hernández J, González GE. 2021. Genome size and repetitive sequences are driven by artificial selection on the length of the vegetative cycle in maize landraces from Northeastern Argentina. *Rodriguesia* 72: e03542018.

102. Revell LJ. 2024. phytools 2.0: an updated R ecosystem for phylogenetic comparative methods (and other things). *PeerJ* 12: e16505.
103. Rice A, Mayrose I. 2021. Model adequacy tests for probabilistic models of chromosome-number evolution. *New Phytologist* 229: 3602–3613.
104. Roa F, Guerra M. 2012. Distribution of 45S rDNA sites in chromosomes of plants: Structural and evolutionary implications. *BMC Evolutionary Biology* 12: 225–238.
105. Roa F, Guerra M. 2015. Non-random distribution of 5S rDNA sites and its association with 45S rDNA in plant chromosomes. *Cytogenetic and Genome Research* 146: 243–249.
106. Ronquist F, Teslenko M, van der Mark P, Ayres DL, Darling A, Höhna S et al. 2012. MrBayes 3.2: efficient Bayesian phylogenetic inference and model choice across a large model space. *Systematic biology* 61: 539–542.
107. Santos GS, Santos AMS, Marques A, Carvalho-Sobrinho J, Lewis GP, Moraes AP, Felix L, Mata-Sucre Y, Andrade MJG, Souza G. 2025. Macroevolutionary trends in the karyotypic evolution of Caesalpinioideae (Leguminosae). *Botanical Journal of the Linnean Society* 00: 1–22.
108. Schliep K, Potts AJ, Morrison DA, Grimm GW. 2017. Intertwining phylogenetic trees and networks. *Methods in Ecology and Evolution* 8: 1212–1220.
109. Schuiteman A, Chase M. 2015. A reappraisal of *Maxillaria* (Orchidaceae). *Phytotaxa* 225: 1–78.
110. Schweizer D. 1976. Reverse fluorescent chromosome banding with chromomycin and DAPI. *Chromosoma* 58: 307–324.
111. Serna-Sánchez MA, Pérez-Escobar OA, Bogarín D, Torres-Jimenez MF, Alvarez-Yela AC, Arcila-Galvis JE, Hall C, Barros F, Pinheiro F, Dodsworth S, Chase M, Antonelli A, Arias T. 2021. Plastid phylogenomics resolves ambiguous relationships within the orchid family and provides a solid timeframe for biogeography and macroevolution. *Scientific Reports* 11: 1–11.
112. Shafir A, Halabi K, Baumer E, Mayrose I. 2025. ChromEvol v.3: modeling rate heterogeneity in chromosome number evolution. *New Phytologist* 245: 1787–1800.
113. Simmons MP, Pickett KM, Miya M. 2004. How meaningful are Bayesian support values? *Molecular Biology and Evolution* 21: 188–199.
114. Singer RB, Koehler S. 2004. Pollinarium morphology and floral rewards in Brazilian Maxillariinae (Orchidaceae). *Annals of Botany* 93: 39–51.
115. Soltis DE, Soltis PS, Bennett MD, Leitch IJ. 2003. Evolution of genome size in the angiosperms. *American Journal of Botany* 90: 1596–1603.
116. Stebbins GL. 1971. Relationships between adaptative radiation, speciation and major evolutionary trends. *Taxon* 20: 3–16.
117. Steenwyk JL, Buida TJ, Lin Y, Shen XX, Rokas A. 2020. ClipKIT: A multiple sequence alignment trimming software for accurate phylogenomic inference. *PLoS Biology* 18: 1–17.
118. Suchard MA, Lemey P, Baele G, Ayres DL, Drummond AJ, Rambaut A. 2018. Bayesian phylogenetic and phylodynamic data integration using BEAST 1.10. *Virus Evolution* 4: vey016.

119. Sun Y, Skinner D. Z, Liang G. H, Hulbert S. H. 1994. Phylogenetic analysis of *Sorghum* and related taxa using internal transcribed spacers of nuclear ribosomal DNA. *Theoretical and Applied Genetics* 89: 26–32.

120. Thiers BM. 2026. Index Herbariorum: A global directory of public Herbaria and associated Staff. New York Botanical Garden. Published online: https://sweetgum.nybg.org/science/ih/.

121. Trávníček P, Čertner M, Ponert J, Chumová Z, Jersáková J, Suda J. 2019. Diversity in genome size and GC content shows adaptive potential in orchids and is closely linked to partial endoreplication, plant life-history traits and climatic conditions. *New Phytologist* 224: 1642–1656.

122. Volleth M, Greilhuber J, Heller KG, Müller S, Yong HS, Loidl J. 2023. Increased genome size is caused by heterochromatin addition in two non-related bat species, *Hesperoptenus doriae* and *Philetor brachypterus* (Vespertilionidae, Chiroptera, Mammalia). *Chromosoma* 132: 269–288.

123. Wanzebock E, Schofer C, Schweizer D, Bachmair A. 1997. Ribosomal transcription units integrated via T-DNA transformation associate with the nucleolus and do not require upstream repeat sequences for activity in *Arabidopsis thaliana*. *The Plant Journal* 11: 1007–1016.

124. Week B, Nuismer SL, Harmon LJ, Krone SM. 2021. A white noise approach to evolutionary ecology. *Journal of Theoretical Biology* 521: 110660.

125. Whitney KD, Garland T. 2010. Did genetic drift drive increases in genome complexity? *PLoS Genetics* 6: e1001080.

126. Whitten WM, Blanco MA, Williams NH, Koehler S, Carnevali GC, Singer RB, Endara L, Neubig KM. 2007. Molecular phylogenetics of *Maxillaria* and related genera (Orchidaceae: Cymbidieae) based on combined molecular dat sets. *American Journal of Botany* 94: 1860–1889.

127. Whitten WM, Williams NH, Chase MW. 2000. Subtribal and generic relationships of Maxillarieae (Orchidaceae) with emphasis on Stanhopeinae: combined molecular evidence. *American Journal of Botany* 87: 1842–1856.

128. Zhang G, Hu Y, Huang MZ, Huang WC, Liu DK, Zhang D et al. 2023. Comprehensive phylogenetic analyses of Orchidaceae using nuclear genes and evolutionary insights into epiphytism. *Journal of Integrative Plant Biology* 65: 1204–1225.

129. Zhao L, Yuan H, Liu X, Chang H, Jing X, Nie Y, Huang Y. 2025. Evolutionary dynamics of repetitive elements and their relationship with genome size in Acrididae. *Genomics* 117: 110971.

Figures

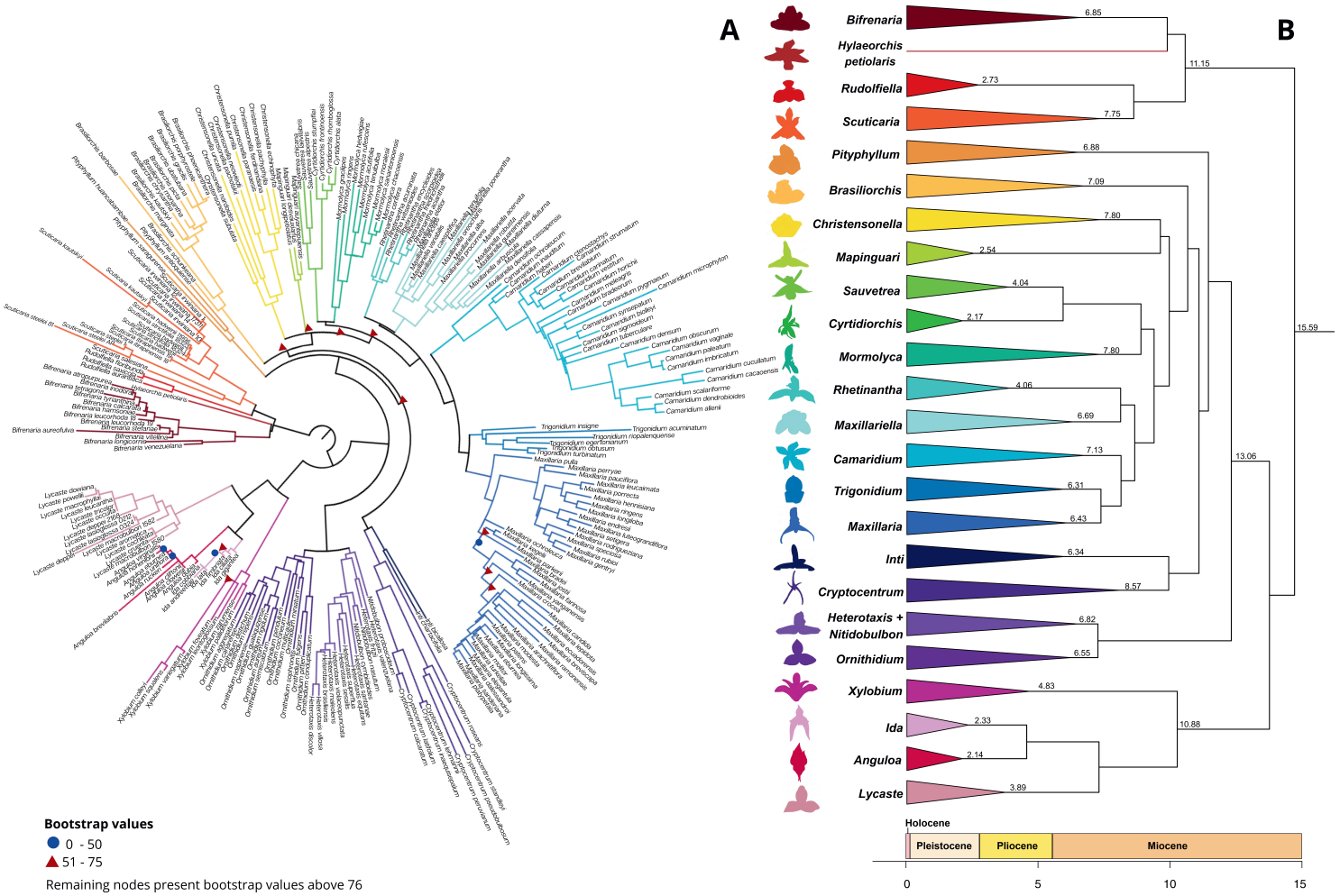


Figure 1

Phylogenetic relationships and divergence-time estimates in Maxillariinae. Genera are indicated by different colours and stylized flowers. (A) Maximum Likelihood topology. Red circles indicate bootstrap support values of 0–50, whereas blue triangles indicate values of 51–75; branches without symbols have support values ≥ 76. (B) Time-calibrated phylogeny of Maxillariinae, with node ages based on height median indicated in million years ago (Mya). The legend indicates geological periods and their corresponding ages in Mya.

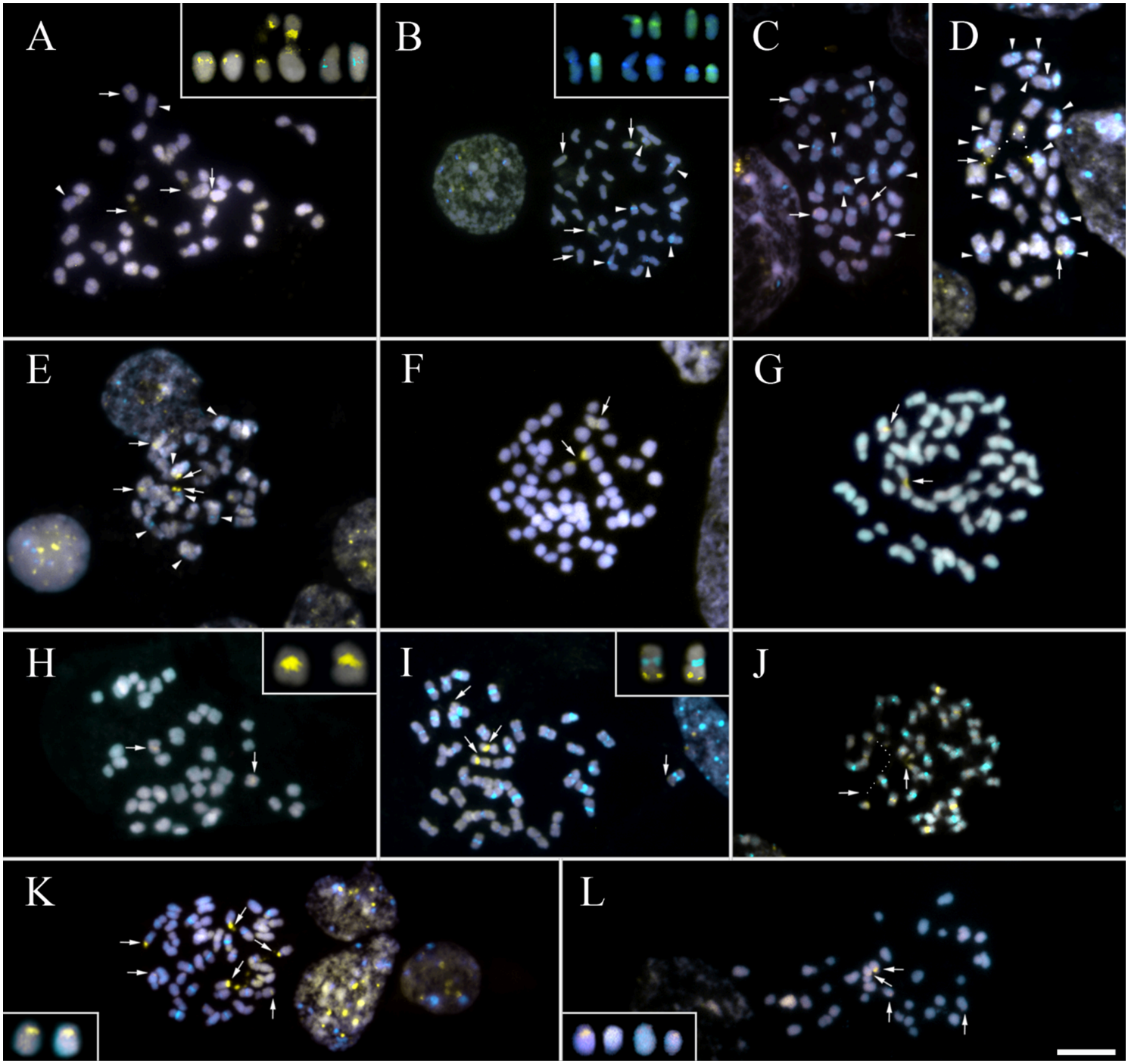


Figure 2

Superimposed images of metaphases after CMA (yellow) / DAPI (blue) banding. (A) *Camaridium ochroleucum* Lindl. (2n = 38); (B) *Maxillaria crocea* Lindl. (2n = 40); (C) *Maxillaria kegelii* Rchb.f. (2n = 40); (D) *Maxillaria ochroleuca* Lodd. ex Lindl. (2n = 40); (E) *Maxillaria spiritu-sanctensis* Pabst (2n = 40); (F) *Maxillariella alba* (Hook.) Blanco and Carnevali (2n = 60); (G) *Maxillariella aff. alba* (Hook.) Blanco and Carnevali (2n = 50); (H) *Maxillariella tenuifolia* (Lindl.) Blanco and Carnevali (2n = 40); (I) *Mormolyca ringens* (Lindl.) Gentil (2n = 40); (J) *Mormolyca rufescens* (Lindl.) Blanco (2n = 40); (K) *Nitidobulbon nasutum* (Rchb.f.) Ojeda and Carnevali (2n = 46); (L) *Rhetinantha cerifera* (Barb.Rodr.) Blanco (2n = 38). Arrows indicate small CMA^+ bands, whereas arrowheads indicate small $DAPI^+$ bands (the total number

of bands is summarised in Table 1). Chromosomes bearing small heterochromatic bands are highlighted in detail in A, B, H, I, K, and L. Dotted lines in (D) and (J) indicate distended CMA^0 bands linking the satellite to the chromosome. The scale bar in (L) indicates 10 μm.

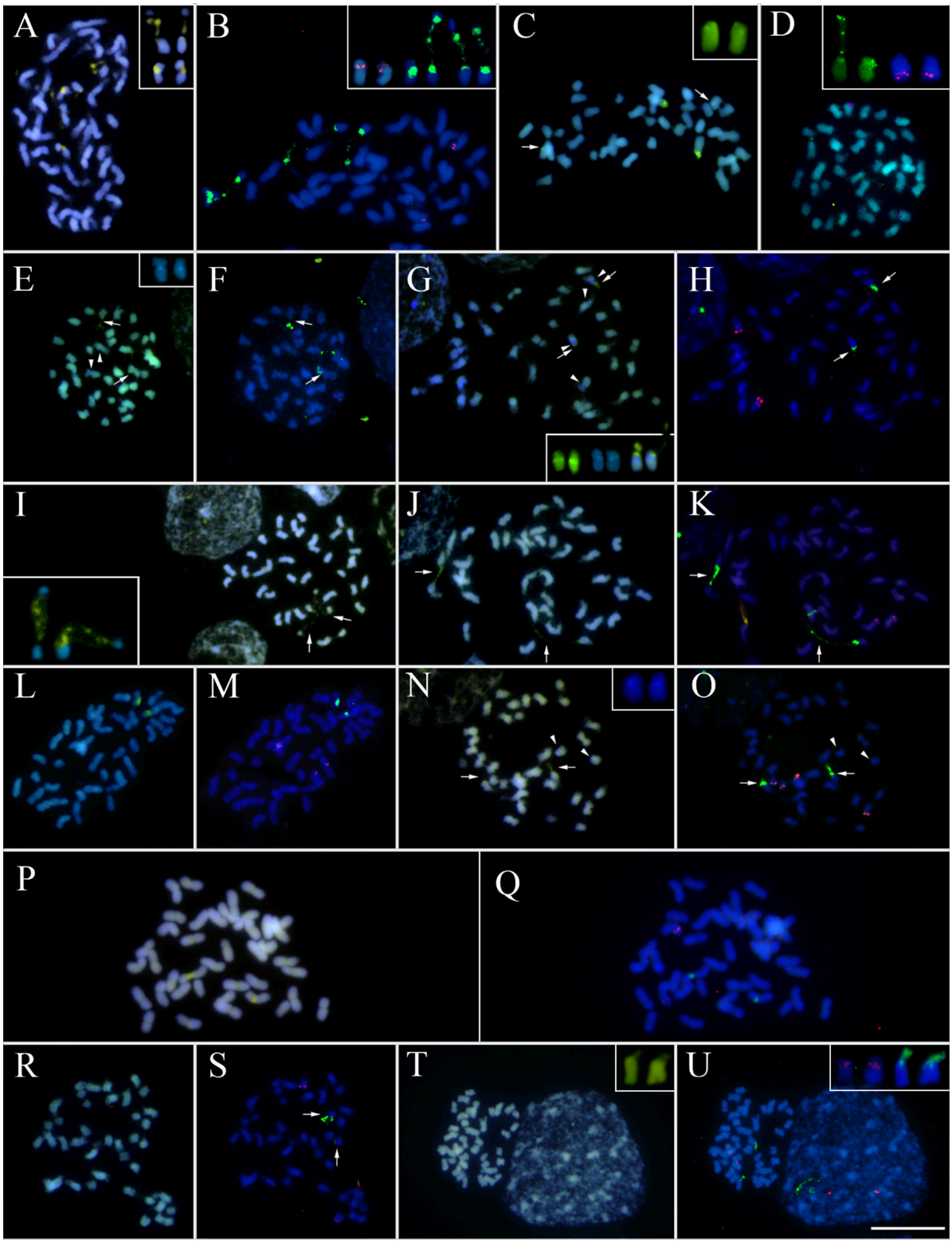


Figure 3

Superimposed images of metaphases after CMA (yellow) / DAPI (blue) banding and *in situ* hybridisation locating 5S and 45S rDNA sites. (A-B) *Brasiliorchis consanguinea* (Klotzsch) R.B.Singer, S.Koehler and Carnevali (2n = 40); (C-D) *Lycaste aromatica* (Graham) Lindl. (2n = 40); (E-F) *Maxillaria bradei* Schltr. ex Hoehne (2n = 40); (G-H) *Maxillaria leucaimata* Barb.Rodr. (2n = 40); (I-K) *Ornithidium adendrobium* (Rchb.f.) Blanco and Ojeda (2n = 38); (L-M) *Maxillariella variabilis* (Bateman ex Lindl.) Blanco and Carnevali (2n = 42); (N-O) *Rhetinantha friedrichsthalii* (Rchb.f.) Blanco (2n = 36); (P-Q) *Scuticaria steelei* (Hook.) Lindl. (2n = 40); (R-S) *Trigonidium acuminatum* Bateman ex Lindl. (2n = 40); (T-U) *Trigonidium obtusum* Lindl. (2n = 40). Panels in A, C, E, G, I, J, L, N, P, R, and U show CMA/DAPI-stained metaphases, whereas the remaining metaphases show in situ hybridisation using 5S (red) and 45S (green) rDNA probes. Dotted line in (I) indicates distended constrictions stained with CMA. Arrows indicate small CMA^+ bands, whereas arrowheads indicate small $DAPI^+$ bands (total number of bands is summarised in Table 1). Chromosomes bearing small heterochromatic bands are highlighted in boxed details. The scale bar in (U) indicates 10 μm.

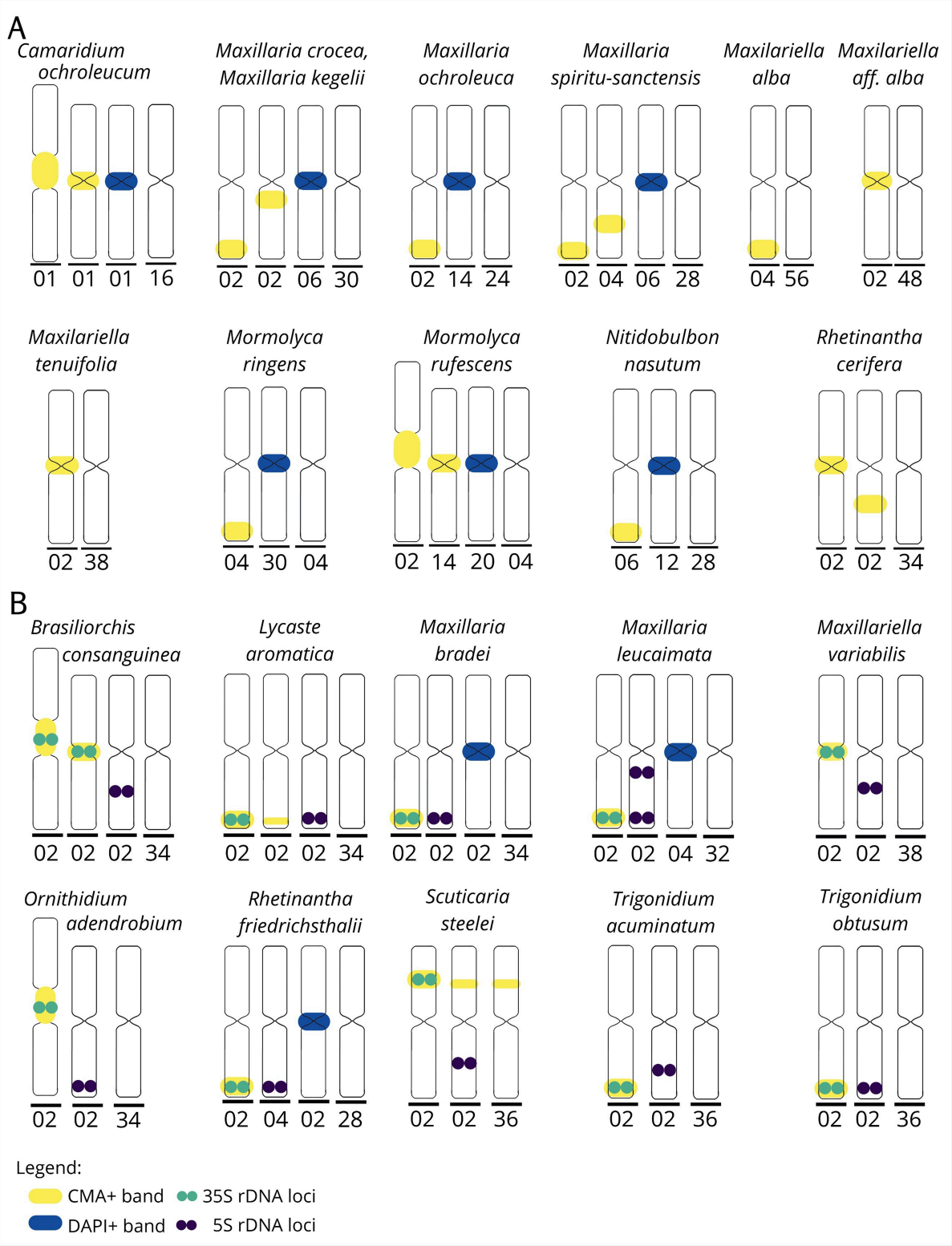


Figure 4

Representative idiograms of selected Maxillariinae species showing variation in chromosome number and in the distribution of heterochromatic bands and ribosomal DNA loci. (A) Distribution of CMA⁺ (yellow) and DAPI⁺ (blue) bands. (B) Distribution of CMA⁺ bands (yellow), 45S rDNA loci (green), and 5S rDNA loci (purple), together with DAPI⁺ bands (blue) when present. Chromosome numbers are indicated

below each idiogram. Chromosomes are arranged according to decreasing size and are not drawn to scale.

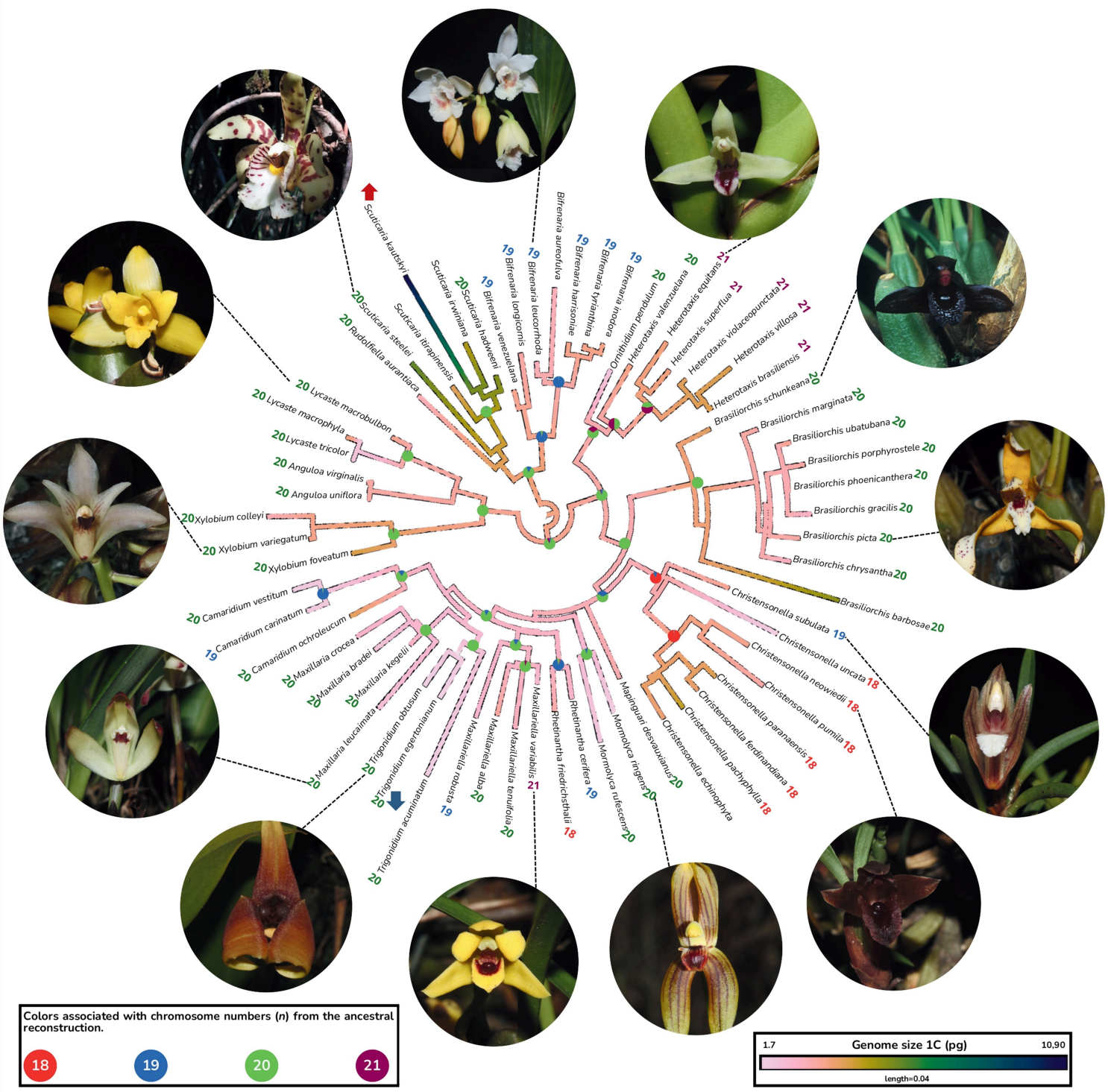


Figure 5

Chromosome number and genome size ancestral reconstruction. The Maxillariinae phylogenetic tree inferred under Maximum Likelihood (ML) was pruned to retain only species for which genome size data were available. Pie charts on the nodes represent the highest probabilities of haploid chromosome numbers inferred from ancestral state reconstruction, with colours corresponding to the values shown in

the legend. The haploid chromosome number detected for each species is indicated next to the species name. For species with more than one chromosome number reported, only the most common chromosome number is indicated. Branches are colored according to genome size (1C, in pg), following the legend. Upward and downward arrows indicate the largest and smallest genome sizes, respectively. Photos: Ana Paula de Moraes.

Supplementary Files

This is a list of supplementary files associated with this preprint. Click to download.

- SupplementaryMaterial.docx
- MoraesetalSupplementaryMaterialTableS1toS9.xlsx
- MoraesetalFigureS1.pdf
- MoraesetalFigureS2.pdf
- MoraesetalFigureS3.pdf
- MoraesetalFigureS4.pdf
- MoraesetalFigureS5.pdf